

Reference: Gragne, A. S., Sharma, A., Mehrotra, R., and Alfredsen, K.: Improving inflow forecasting into hydropower reservoirs through a complementary modelling framework, Hydrol. Earth Syst. Sci. Discuss., 11, 12063-12101, doi:10.5194/hessd-11-12063-2014, 2014.

Dear Editor - dear Dr. Toth,

We would like to thank you again for favourably receiving our manuscript for publication subject to minor revision and contribution to improve quality of the manuscript.

In this round of review, we received positive and critical comments from an anonymous reviewer whom we thank very much for contributing to improve quality of the manuscript.

We acknowledge the mistake we made in selecting the right PIT plot and apologize for that. We have reproduced the appropriate plots and have revised sections of the manuscript to interpret and accommodate insights from the plots.

In the following we present the comments from the editor and an anonymous reviewer, our responses to the issues raised, and the changes made to the manuscript.

Editor

Comments:

1. [...] I believe that the correct number of points in Figure 10 should be the number of hourly data in each season for the entire validation period (5 hydrological years), so around 450×24 (10800 hours) points, and indeed in Figure 10 there seem to be much less dots: can you please explain it?

We thank you (Dr. Toth) for the critical observation and apologize for the mistake. We have produced the appropriate PIT plots and replaced the figure in the revised document (Figure 9). We have revised section 3 of the manuscript in revised version.

Revised Manuscript, Section 3, Page 19 (Line 17-33) - Page 20 (Line 1-10):

The two issues at stake here are the Gaussian assumption on the basis of which the prediction bounds were constructed, and the model identification and parameter estimation approach implemented. In order to assess the former, we conducted the PIT uniformity probability test. From operational hydrology point of view, we concur with the opinion of Thyer et al. (2009) that the toughest goodness-of-fit test the complementary framework has to pass is whether the predictive distribution is consistent with the observed inflow, which the PIT uniform probability plots evaluate directly. At each time step we derived p-value of the observation from the corresponding predictive distribution and constructed empirical cdf of the p-values (i.e. different sets based on season, lead-time, etc.). Comparison of these empirical cdf of the p-values with that of a uniform distribution (Fig. 9c-f) reveal that the uncertainty attached to the deterministic forecasts is imperfect. Overall, PIT uniformity probability test confirms that the uncertainty is overestimated significantly irrespective of season and lead-time. In relative terms, significance of the overestimation reduces with increased lead-time. PIT plots of the spring season show a relatively lower uncertainty overestimation, even though they neither plot along the diagonal bisector nor remain within the Kolmogorov 5%. This might explain that the cause of the uncertainty overestimation could be use of a high standard deviation relative to the inflow magnitude occurring throughout the year. However, this finding of “uncertainty overestimation” clearly contradicts the lower than expected percentage of coverage the CR metrics revealed. This along with evidences of the need to truncate the lower tails of the prediction bound, and recalling from the Kolmogorov-Smirnov test (section 3.3) that the residuals from the error forecasting model did not honour the homoscedasticity assumption even after transformation, might suggest invalidity of the model assumption. According to Schoups and Vrugt (2010), in hydrologic applications residual series are often assumed to be independent and identically distributed but these assumptions are usually violated. In the next section, we briefly assess reliability of the model identification and parameter estimation approach implemented in this study.

The PIT uniform probability plots revealed that both approaches significantly overestimated the uncertainty in a similar pattern. Comparison of the CR of the GML and LS-LK based models showed a similar proportion of observations contained in the prediction interval. The CR again reveals the same characteristics of high values at short lead-times and the fraction of observations contained in the prediction bound declines at longer lead-times. This affirms that validity of the Gaussian assumptions stand out as the main issue requiring further investigation in relation to probabilistic assessment.

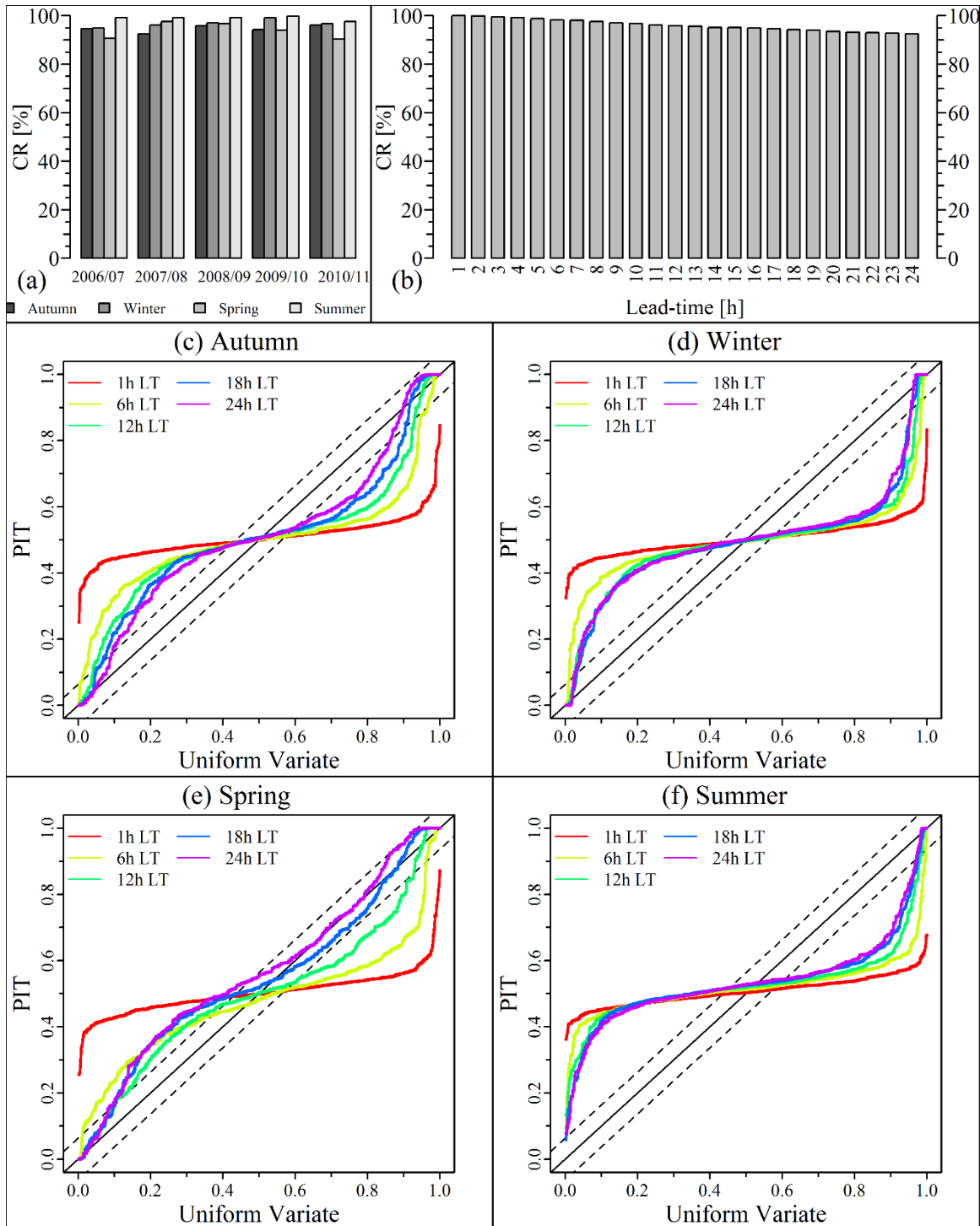


Figure 9. Reliability score (containing ratio-CR) for 95% prediction interval for: (a) each season of every hydrologic year; and (b) different forecast lead-times based on entire series. Panels (c)-(f): sample PIT uniform probability plots for each of the four seasons at 1, 6, 12, 18 and 24 hour forecast lead-times. Solid line

designates the theoretical uniform distribution, broken lines represent the Kolmogorov significance band, and the dots denote PIT value of the observed p-values.

Anonymous Referee

Comments:

1. I suspect that the PIT plots in Figure 10 are incorrect.

We thank the anonymous referee for the critical observation and accept with apology that we had erred in producing the appropriate plots. We have now replaced them with the correct plots (Figure 9). In the following we respond to the two points (a & b in the reverse order) the anonymous reviewer raised in relation to the PIT plots for the sake of outlining the method we adopted clearly.

b) I am not sure how the authors generated ensemble forecasts to make PIT plots, especially for the 24h LT forecasts. I only can see the deterministic forecasts defined by Equation (3) and the forecast interval estimated by LRVE (Page 10 Line 7). The forecast interval only provides information on forecast spread but the PIT plots provide more. Can you elaborate on how to generate the PIT plots from the forecast intervals?

In line with the reviewer's observation, the approach we followed is not ensemble based. Since our attempt has been to mimic the operational practice in the Norwegian hydropower industry, the overall approach we preferred in this study has been producing probabilistic forecasts based on deterministic forecasts. Hence, in order to derive the PIT plots, we relied on the statistical properties we used for quantifying the 95% prediction bound and the Gaussian assumption. At each forecast time step we generated 100 forecasts and the corresponding predictive distribution from which we derived the p-value corresponding to the observation (Figure A1). Subsequently, we collected the p-values over the selected set (e.g. lead-time of 1,2,...,24 of different seasons) to construct the respective empirical cdf, which we compared with cdf of a uniform distribution (Figures A2-A11).

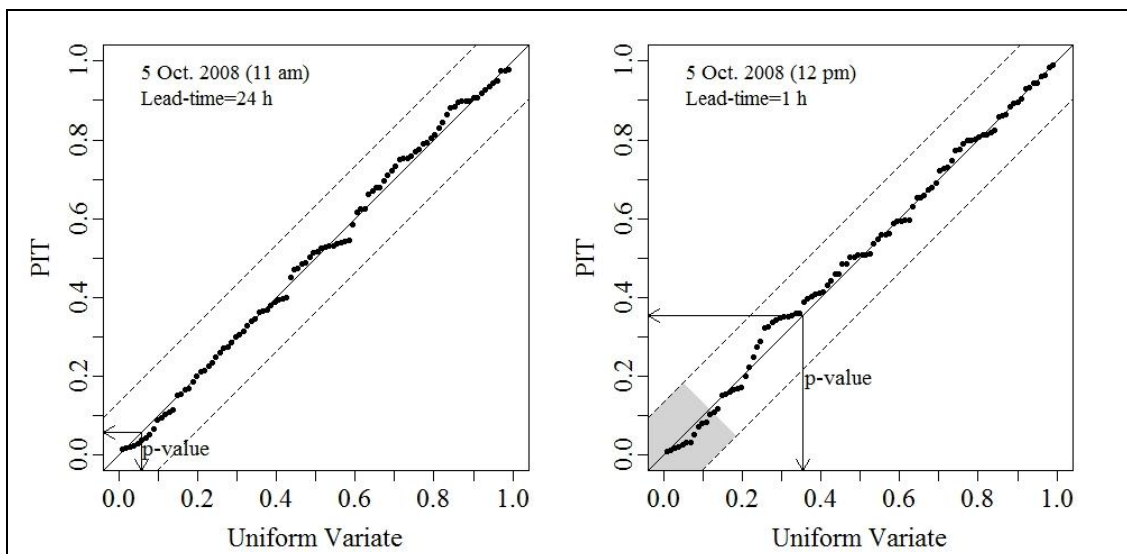


Figure A1. Example PIT uniform probability plots of the inflow ensembles at selected forecast time steps. The grey shaded area in the right panel designates region of the predictive distribution

where the generated forecasts are unrealistic (inflows of magnitudes less than zero). The arrows point to the p -value corresponding to the observation.

- a) The number of points in the PIT plots is not consistent with the number of hourly-data in the validation period. The case study uses four-year data in the validation period. That makes the number of the total hourly data is ~ 35040 or ~ 8760 per season. If the forecast system issues one forecast per day, there should be around 365 points in each PIT plot. Based on my visual inspection, there are much fewer points in the plot. In addition, based on the Kolmogorov critical value is ~ 0.25 for each plot and the approximation of critical value (critical level is 0.95) for the Kolmogorov test is $1.358/\sqrt{n}$, I estimate that only ~ 30 points are available in each plot. I suggest you use all hourly data (~ 8760 per season) to construct PIT plots.

We agree with the reviewer that the PIT plots in the previous manuscript displayed much fewer points than they should. As stated early on in this response letter, they were incorrect plots similar to those presented in Figure A1 (but only with 40 ensembles) than proper PIT plots desired for the current purpose, which are shown in Fig. 9(c-f) and A2-A11.

2. Some of Figure numbers are not updated. For example, (Page 13 Line 13) Fig. 4a should be Fig 5.

We thank the reviewer for the observation and apologize for the oversight from our side. We have noted that the figure numbers in the marked-up version of the previous manuscript began from 2 instead of 1; now fixed.

In addition to the above changes, we have added a reference to a subsequent work (Gragne et al., 2015) we believe will lead readers to one approach to deal with the challenges outlined in the last section.

Revised Manuscript, Section 4, Page 22 (Line 24-28):

A subsequent work (Gragne et al., 2015) attempts to address some of these issues using a filter updating procedure, which assimilates inflow measurements periodically to the error-forecasting model, and explores the potential of a data assimilation technique for improving model forecast accuracy and constraining forecast uncertainty without significant computational costs.

We would be happy to answer any further question!

Best regards,

Ashenafi S Gragne (corresponding author)

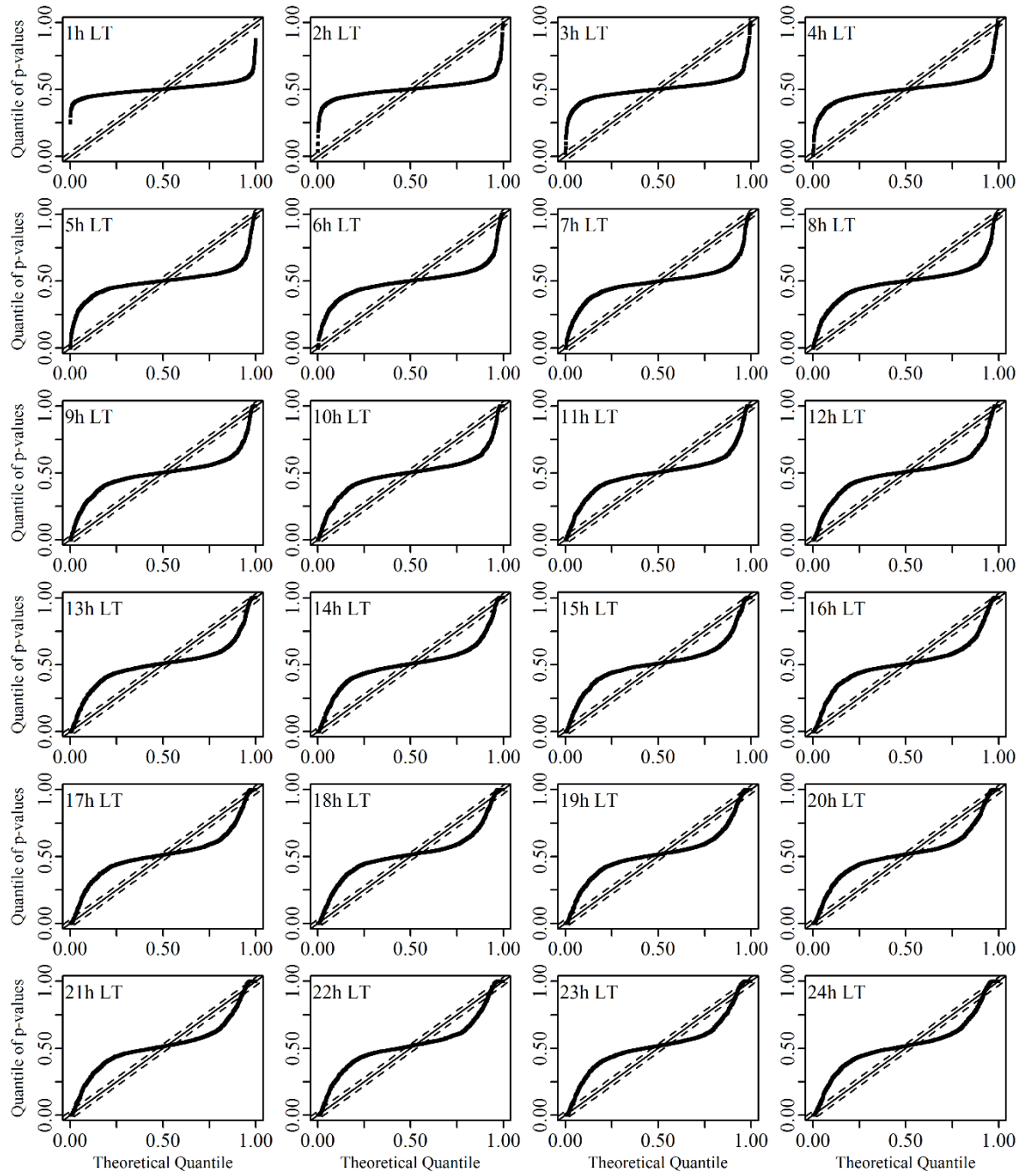


Figure A2. PIT uniform probability plot (entire data set; LS-KS (present) approach).

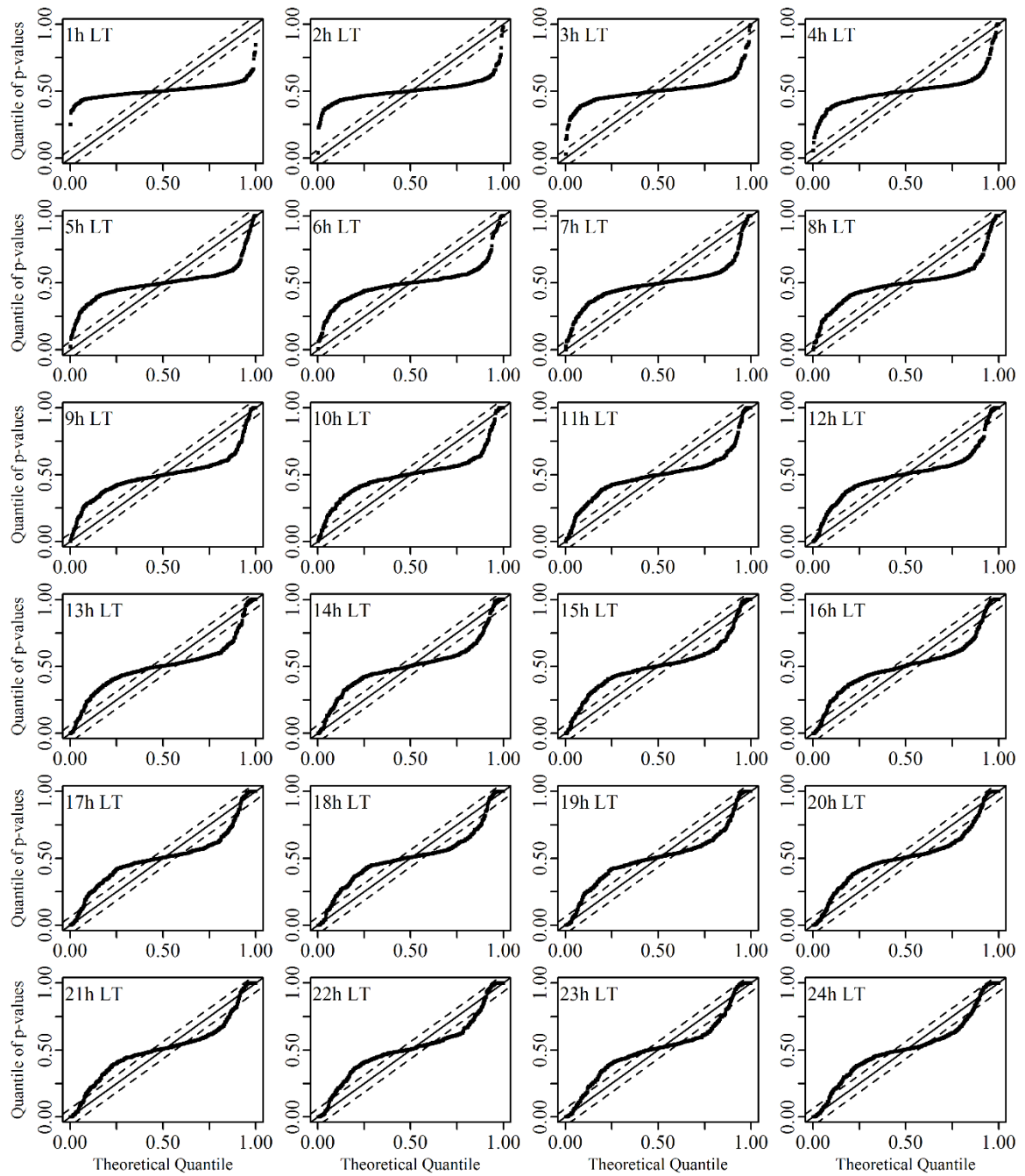


Figure A3. PIT uniform probability plot (autumn set; LS-KS (present) approach).

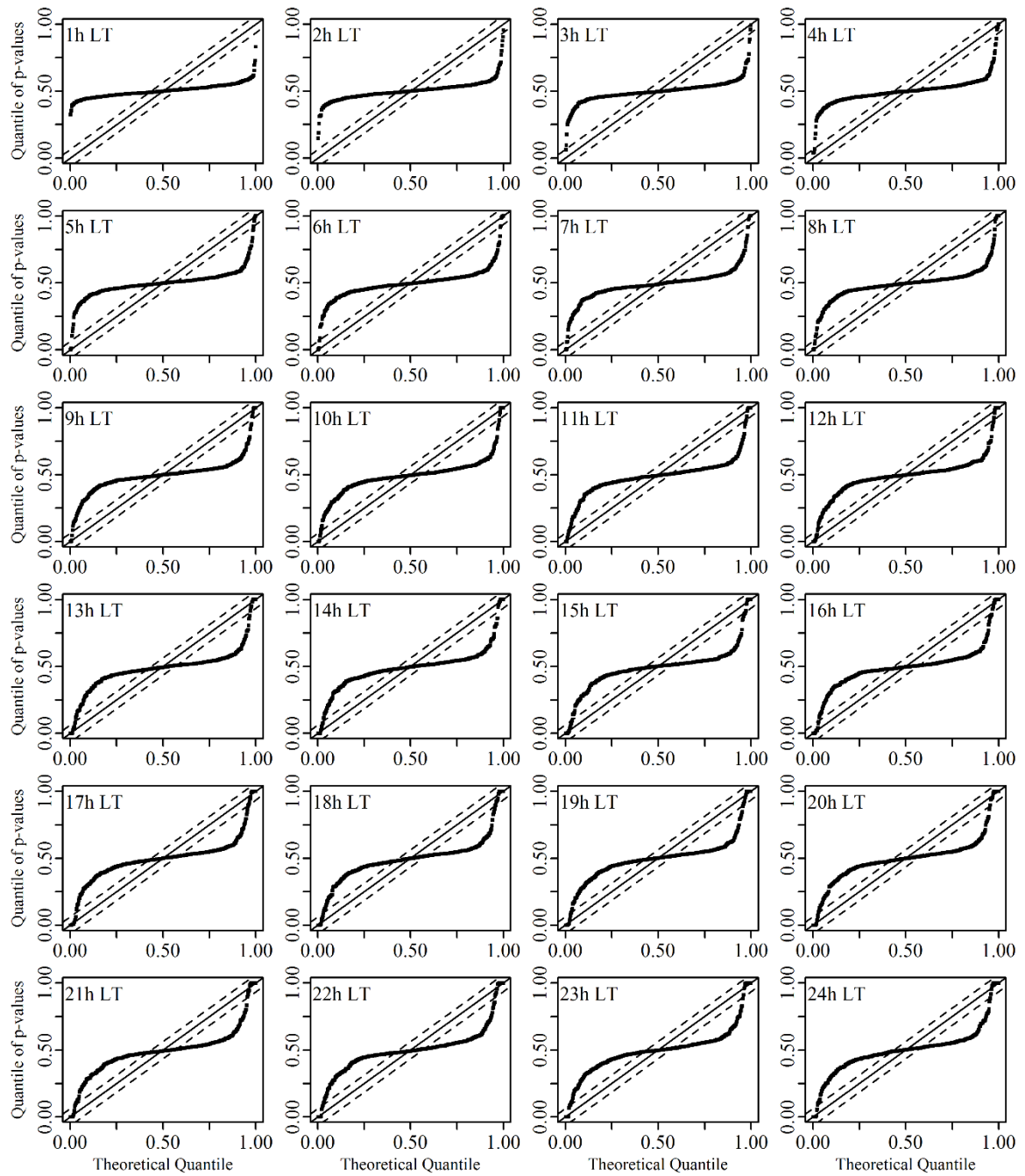


Figure A4. PIT uniform probability plot (winter set; LS-KS (present) approach).

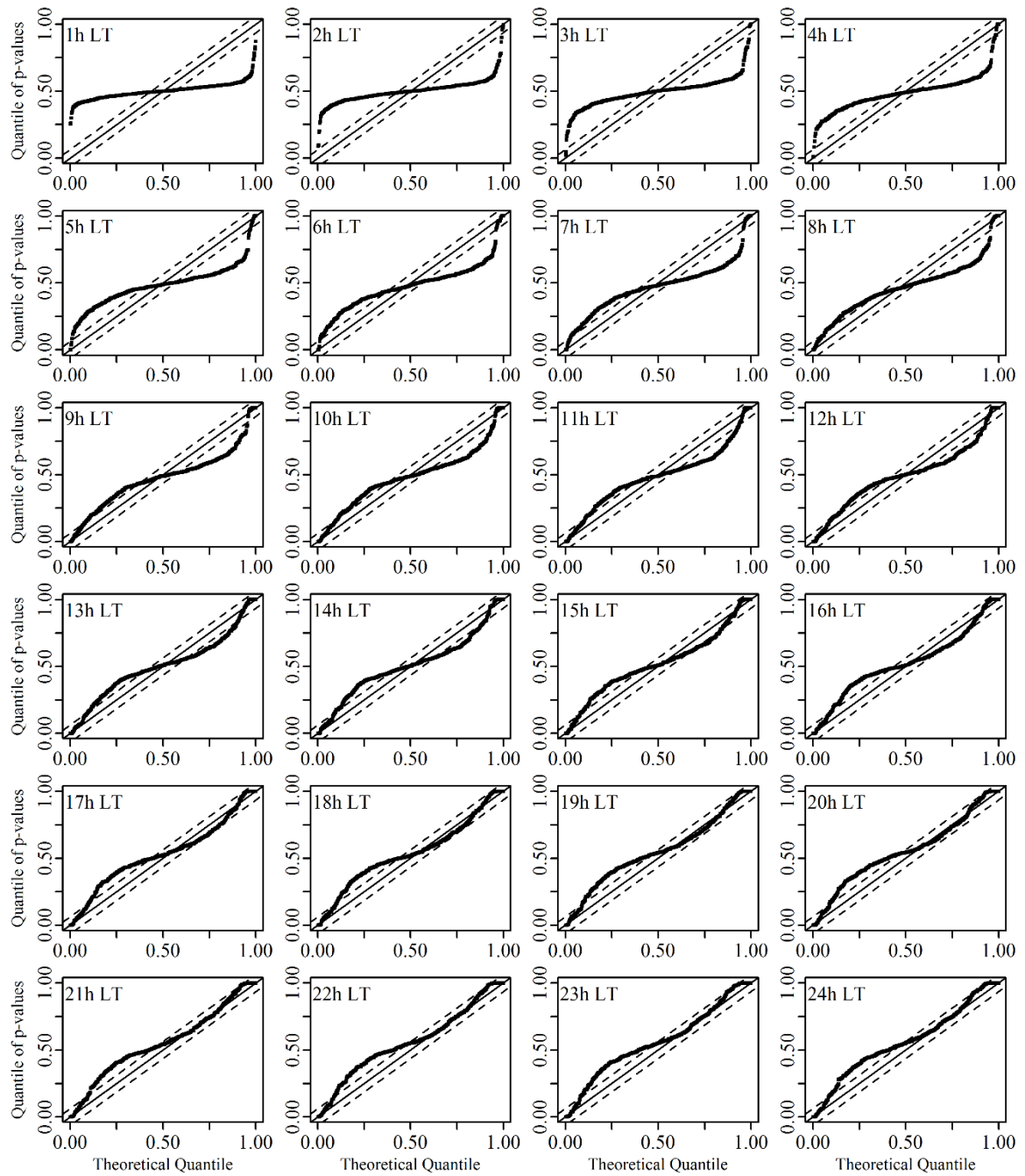


Figure A5. PIT uniform probability plot (spring set; LS-KS (present) approach).

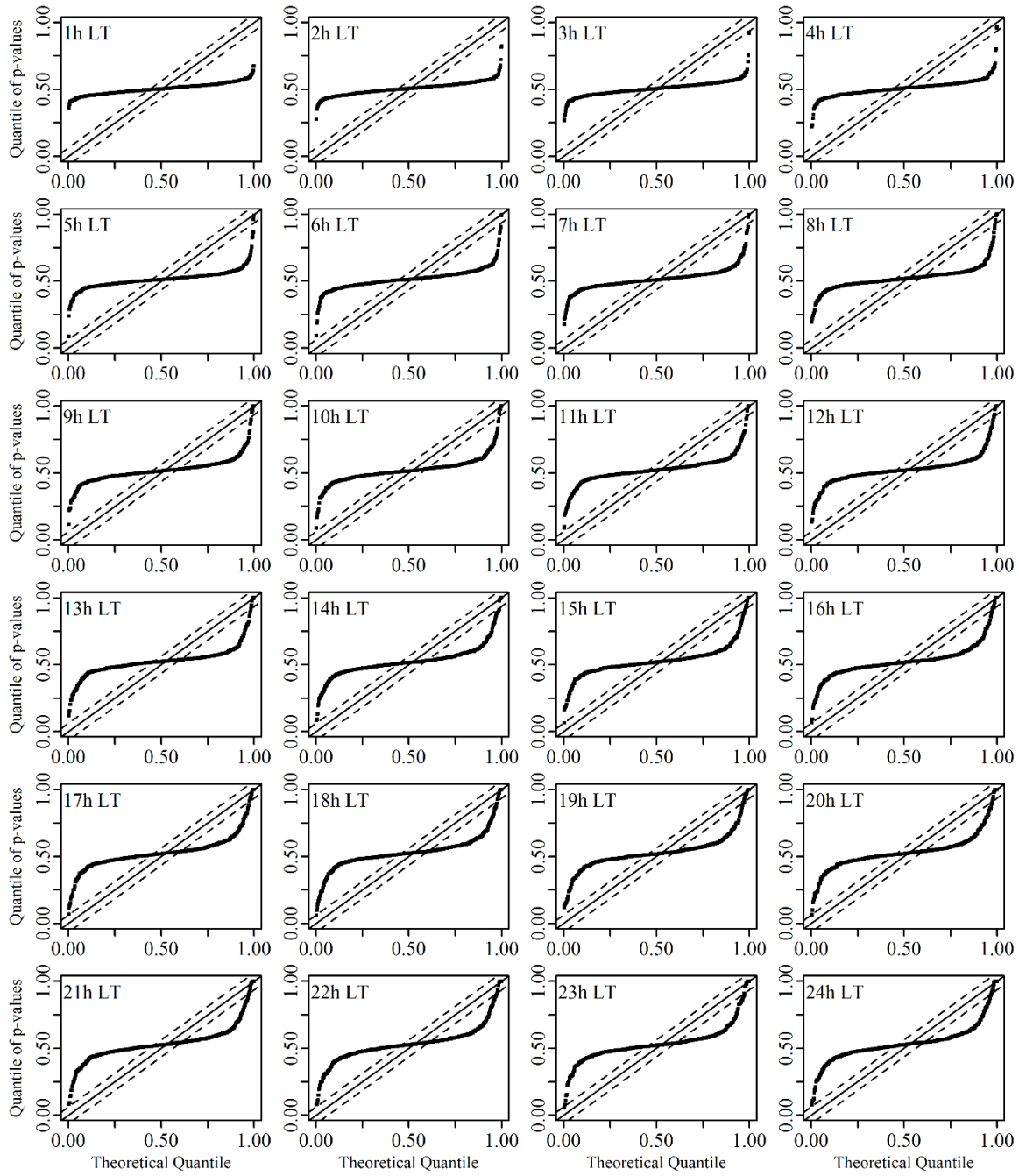


Figure A6. PIT uniform probability plot (summer set; LS-KS (present) approach).

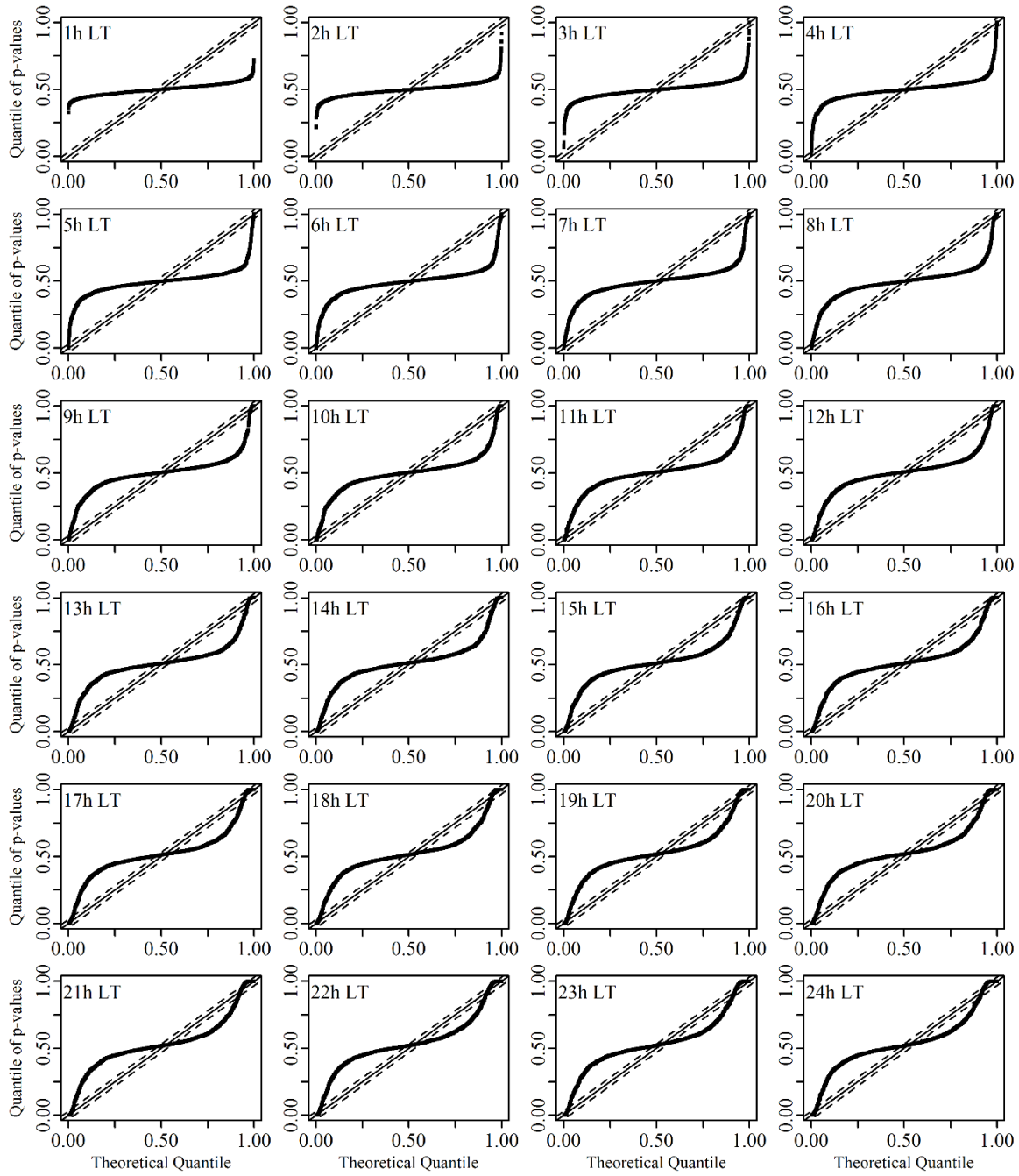


Figure A7. PIT uniform probability plot (entire data set; GML approach).

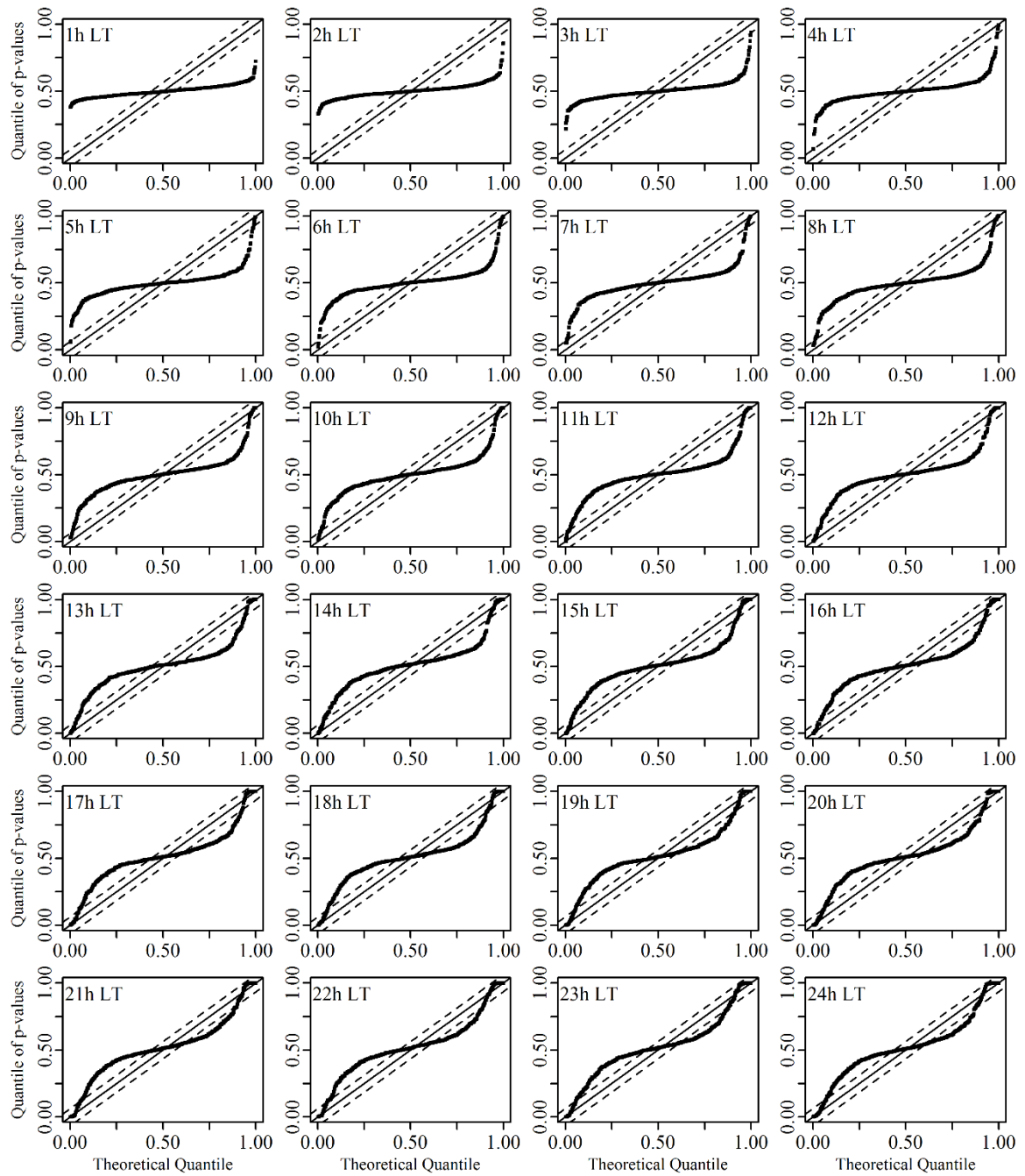


Figure A8. PIT uniform probability plot (autumn set; GML approach).

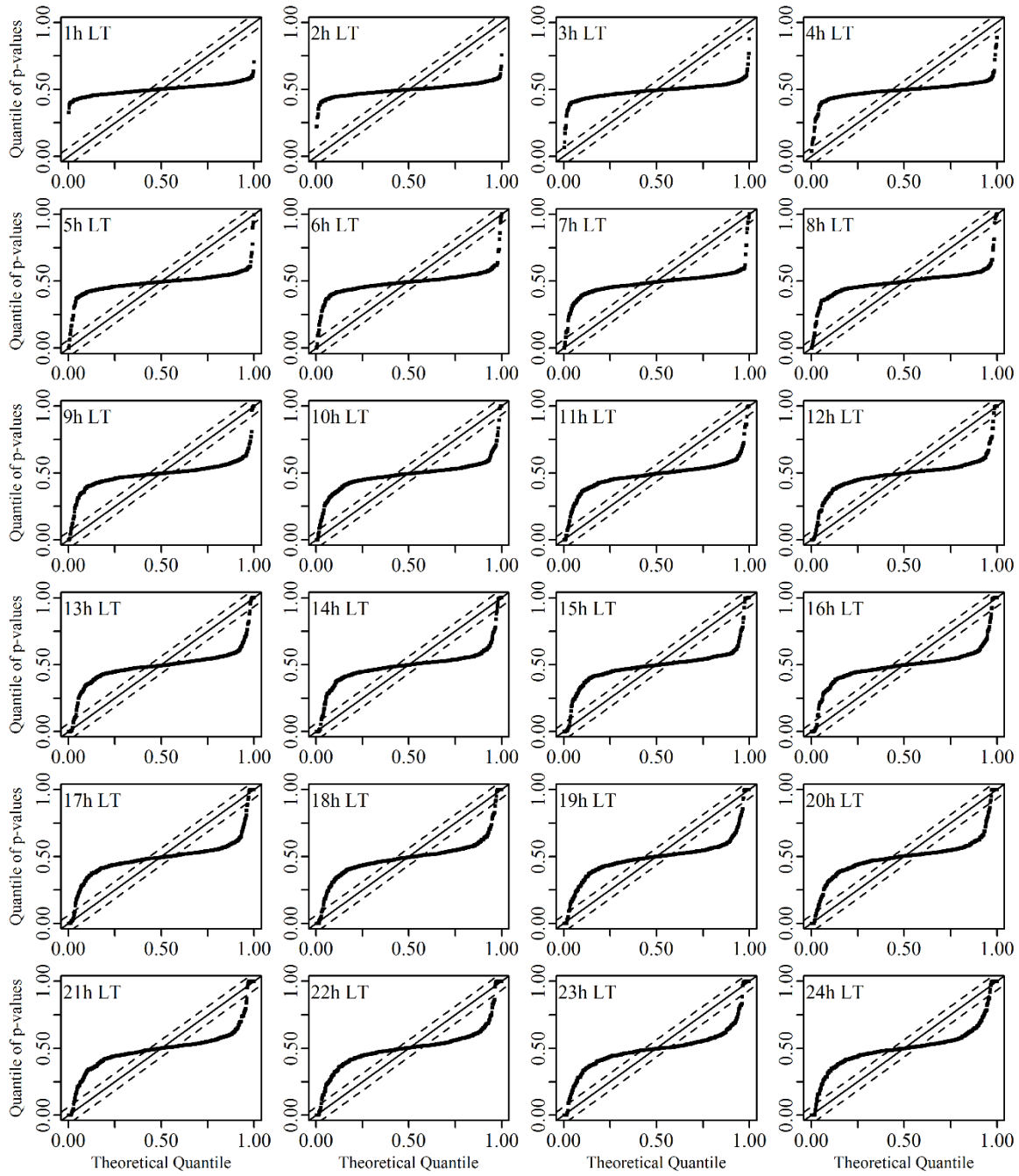


Figure A9. PIT uniform probability plot (winter set; GML approach).

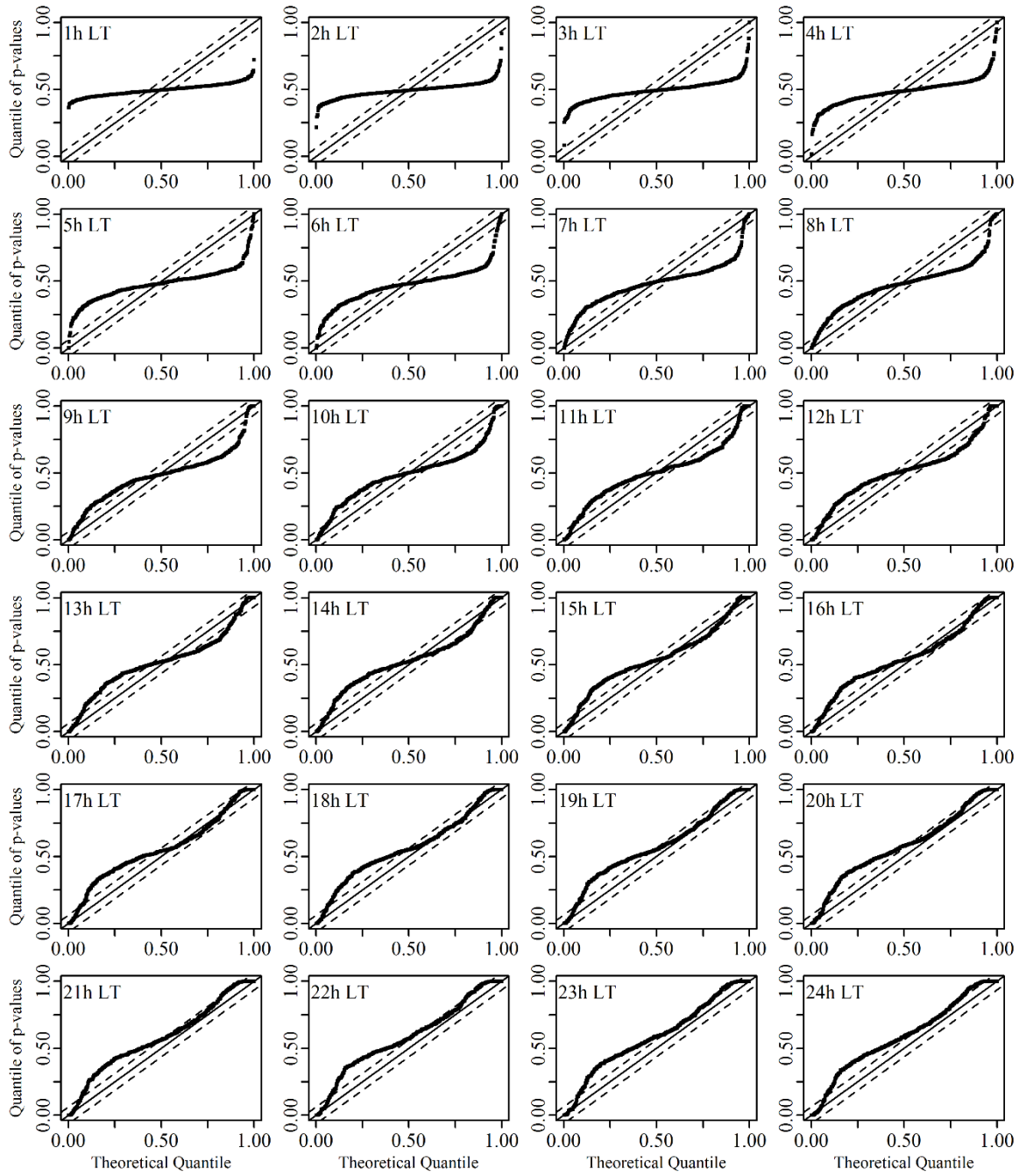


Figure A10. PIT uniform probability plot (spring set; GML approach).

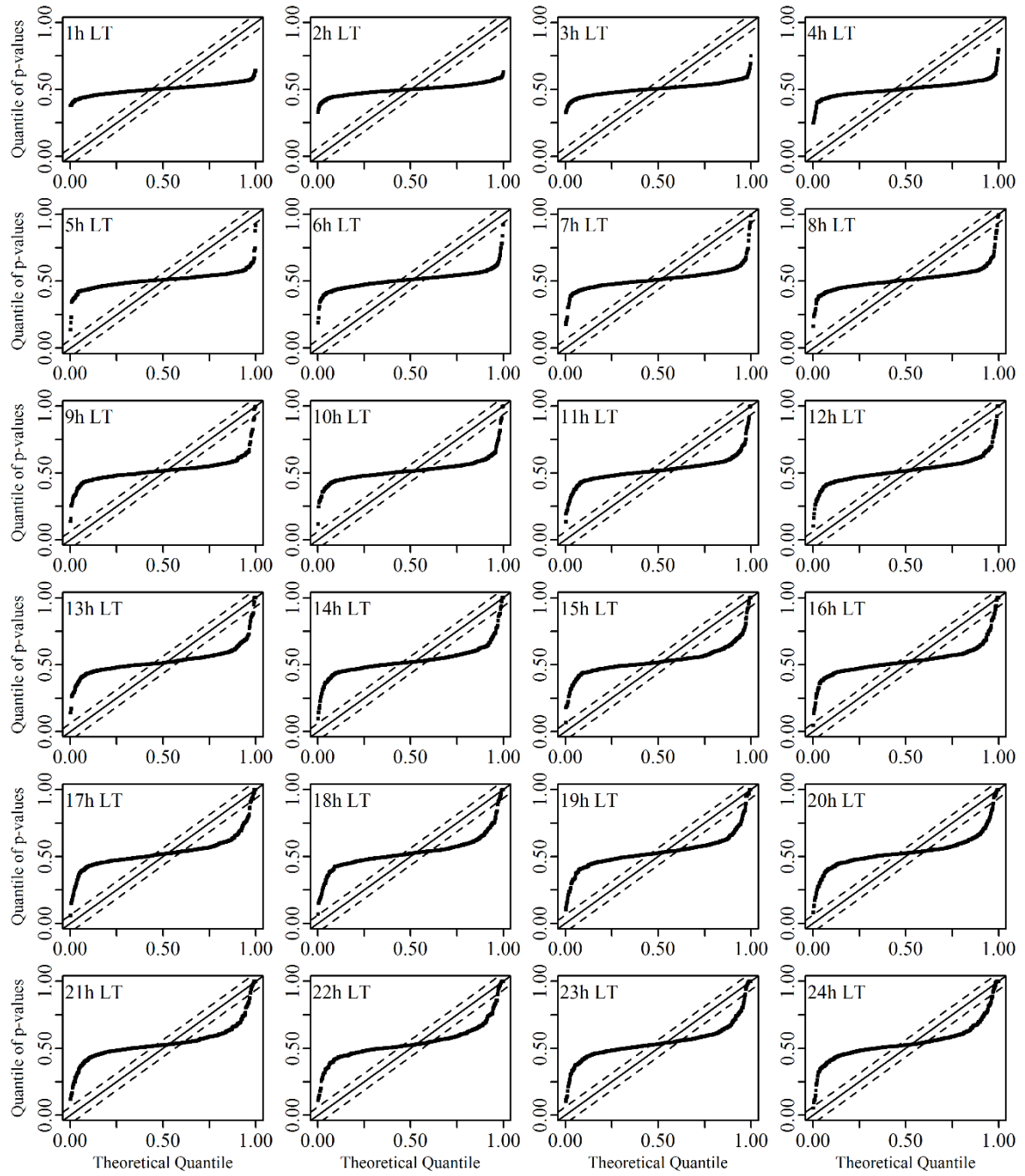


Figure A11. PIT uniform probability plot (summer set; GML approach).

1 Improving real-time inflow forecasting into hydropower 2 reservoirs through a complementary modelling framework

3
4 **A. S. Gragne¹, A. Sharma², R. Mehrotra² and K. Alfredsen¹**

5 [1]{Department of Hydraulic and Environmental Engineering, Norwegian University of
6 Science and Technology, Trondheim, Norway}

7 [2]{School of Civil and Environmental Engineering, The University of New South Wales,
8 Sydney, Australia}

9 10 **Abstract**

11 Accuracy of reservoir inflow forecasts is instrumental for maximizing the value of water
12 resources and benefits gained through hydropower generation. Improving hourly reservoir
13 inflow forecasts over a 24 hour lead-time is considered within the day-ahead (Elspot) market
14 of the Nordic exchange market. A complementary modelling framework presents an approach
15 for improving real-time forecasting without needing to modify the pre-existing forecasting
16 model, but instead formulating an independent additive or complementary model that captures
17 the structure the existing operational model may be missing. We present here application of this
18 principle for issuing improved hourly inflow forecasts into hydropower reservoirs over
19 extended lead-times, and the parameter estimation procedure reformulated to deal with bias,
20 persistence and heteroscedasticity. The procedure presented comprises an error model added
21 on top of an un-alterable constant parameter conceptual model, the models being demonstrated
22 with reference to the 207 km² Krinsvatn catchment in central Norway. The structure of the error
23 model is established based on attributes of the residual time series from the conceptual model.
24 Besides improving forecast skills of operational models, the approach estimates the uncertainty
25 in the complementary model structure and produces probabilistic inflow forecasts that entrain
26 suitable information for reducing uncertainty in the decision-making processes in hydropower
27 systems operation. Deterministic and probabilistic evaluations revealed an overall significant
28 improvement in forecast accuracy for lead-times up to 17 hours. Season based evaluations
29 indicated that the improvement in inflow forecasts varies across seasons and inflow forecasts

1 in autumn and spring are less successful with the 95% prediction interval bracketing less than
2 95% of the observations for lead-times beyond 17 hours.

3

4 **1 Introduction**

5 Hydrologic models can deliver information useful for management of natural resources and
6 natural hazards (Beven, 2009). They are important components of hydropower planning and
7 operation schemes where it is essential to estimate future reservoir inflows and quantify the
8 water available for power production on a daily basis. The identification and representation of
9 the significant responses of hydrologic systems have been diverse among hydrologists.
10 Different hydrologists have incorporated their perceptions of the functioning of hydrologic
11 systems into their models and come up with several rival models; some of them process based
12 and others data-based (for thorough reviews of the historic development of hydrologic
13 modelling refer to Todini, 2007 and Beven, 2012). These models can be grouped in to two main
14 classes, conceptual and data-driven models.

15 Lumped conceptual hydrologic models are the most commonly used models in operational
16 forecasting. Models of this class use sets of mathematical expressions to provide a simplified
17 generalization of the complex natural processes of the hydrologic systems in the headwater
18 areas of reservoirs. Application of such models conventionally requires estimating the model
19 parameters by conditioning to observed hydrologic data. Unlike conceptual models, data-driven
20 models establish mathematical relationship between input and output data without any explicit
21 attempt to represent the physical processes of the hydrologic system. Reconciling the two
22 modelling approaches and combining the advantages of both approaches (Todini, 2007), has
23 produced some example applications in forecasting systems where the two modelling
24 approaches are harmoniously used for improving reliability of hydrologic model outputs (e.g.
25 Abebe and Price, 2003 and Solomatine and Shrestha, 2009).

26 Usefulness of a model for operational prediction is determined by the level of accuracy to which
27 the model reproduces observed hydrologic behaviour of the study area. In operational
28 applications, evaluation of how well the models capture rainfall-runoff processes, especially
29 the snow accumulation and melting process in cold regions, is important because the extent to
30 which the models accurately reproduce the reservoir inflows can significantly influence the
31 efficiency of the hydropower reservoir operation and subsequently the power price. Application
32 of hydrologic models for reproducing historic records can suffer from inadequacy in model

1 structure, incorrect model parameters, or erroneous data. Consequently, despite failing to
2 reproduce the observed hydrographs exactly, they enable simulation of hydrologic
3 characteristics of a study catchment to a fair degree of accuracy. It gets more challenging when
4 using the models in the operational setup for forecasting the unknown future just based on the
5 known past, which the model might not capture accurately. In the context of the Norwegian
6 hydropower systems, being unable to predict future reservoir inflows accurately has negative
7 consequences to the power producers. Norway's energy producers have to pledge the amount
8 of energy they produce for next 24 hours in the day-ahead market and if unable to provide the
9 pledged amount of energy the chance of incurring losses is very high. Estimation of future
10 reservoir inflows (be it long- or short-term) involves estimating the actual (initial) state of the
11 basin, forecasting the basin inputs during the lead-time, and describing the water movement
12 during the lead-time (Moll, 1983). Hence, the quality of a hydrologic forecast depends on the
13 accuracy achieved and methodology selected in implementing each of these aspects.

14 In this study, we intend to use conceptual and data-driven models complementarily. A
15 conceptual model with calibrated model parameters is used as the fundamental model that
16 approximately captures dominant hydrologic processes and forecasts behaviour of the
17 catchment deterministically. A data-driven model is then formulated on the residuals, the
18 difference between observations and predictions from the conceptual model. By studying the
19 whole set of residuals and exploring the information they contain, important information that
20 describes the inadequacies of the conceptual model can be extracted. In general, this kind of
21 information can be used for improving either the conceptual model itself or the prediction skill
22 of a forecasting system. Emulating the practice in most Norwegian hydropower reservoir
23 operators, we stick to the latter purpose with the aim of enhancing the performance of a
24 hydropower reservoir inflow forecasting system. According to Kachroo (1992), data-driven
25 models defined on the residuals from a conceptual model can expose whether the conceptual
26 model is adequate to identify essential relationships exhibited in the input-output data series.
27 Data-driven models can establish the mathematical relationship that describes the persistence
28 revealed in the residual time series, which is caused by failure of the conceptual model to
29 capture all the physical processes exactly. Thus, in the operational sense, the data driven models
30 can play a complementary role by adjusting output of the conceptual model whenever the
31 conceptual model needs corrective adaptation (e.g. Serban and Askew, 1991 and
32 World Meteorological Organization, 1992).

1 Several example applications can be found in the scientific literature on using conceptual and
2 data driven models complementarily. For instance, Toth et al. (1999) compared performance
3 improvements six ARIMA based error models brought to streamflow forecasts from a
4 conceptual model to identify the best error model and data requirements. Shamseldin and
5 O'Connor (2001) coupled a multi-layer neural network model on top of a conceptual rainfall-
6 runoff model to improve accuracy of stream flow forecasts without interfering with operation
7 of the conceptual model. Similarly, Madsen and Skotner (2005) developed a procedure for
8 improving operational flood forecasts by combining error models (linear and non-linear) and a
9 general filtering technique. Xiong and O'Connor (2002) investigated performance of four error-
10 forecast models namely, the single autoregressive, the autoregressive threshold, the fuzzy
11 autoregressive threshold and the artificial neural network updating models, for improving real-
12 time flow forecasts and compared their results. Likewise, Goswami et al. (2005) examined the
13 forecasting skill of eight error-modelling based updating methods. A recent review on the
14 application of error models and other data assimilation approaches for updating flow forecasts
15 from conceptual models can be found in Liu et al. (2012).

16 As reviewed above, the principle of complementing conceptual models with data-driven models
17 has enjoyed applications in real-time hydrologic forecasting since the 1990s. The
18 methodological contribution of the present work is reformulation of the parameter estimation
19 procedure for the data-based model. We recognize that the bias, persistence and
20 heteroscedasticity seen in the residuals from the conceptual model reflect structural inadequacy
21 of the conceptual model to capture the catchment processes and, hence, are important in
22 defining the manner the residual series is dealt with. Accordingly, we describe the reservoir
23 inflows in a transformed space and present an iterative algorithm for estimating parameters of
24 the data-driven model and the transformation parameters jointly.

25 Two main features distinguish application aspects of the present paper from previous published
26 works built on the same concept of complementing conceptual models with data driven models.
27 Firstly, it attempts to provide hourly reservoir inflows of improved accuracy 24 hours ahead.
28 The earlier papers mainly succeeded in improving forecasts for forecast lead-times up to six
29 time steps or incorporated a scheme to update the forecast system at an interval of six time-
30 steps. Secondly, an attempt is made in what follows, to produce a probabilistic forecast by
31 estimating the uncertainty of the error model, rather than only the deterministic estimate. This,
32 thereby, enables forecast of an ensemble of reservoir inflows, thereby allowing a risk-based

1 paradigm for hydropower generation being put to use. Reasons as to why hydrologic forecasts
2 should be probabilistic, and the potential benefits therein are presented and explained in
3 Krzysztofowicz (2001). Krzysztofowicz (1999) describes a methodology for probabilistic
4 forecasting via a deterministic hydrologic model. Li et al. (2013) provide review of scientific
5 papers that provide various regression and probabilistic approaches for assessing performance
6 of hydrologic models during calibration and uncertainty assessment. Smith et al. (2012)
7 demonstrate a good example of producing probabilistic forecasts based on deterministic
8 forecast outputs. In this paper, the improvement levels achieved are evaluated deterministically
9 using the same or similar metrics as past studies, and probabilistically using: (i) the containing
10 ratio (Xiong et al., 2009), which is also referred to as reliability score (e.g. Renard et al., 2010);
11 and (ii) the probability integral transform (PIT) plot, which Thyer et al. (2009) refer to as the
12 predictive QQ plot. We here emphasise that taking into account uncertainties emanating from
13 various recognized sources and describing the degree of reliability of the inflow forecasts has
14 important benefits. According to Montanari and Brath (2004), the Bayesian forecasting system
15 (BFS) and the generalized likelihood uncertainty estimation (GLUE) are the popular methods
16 for inferring the uncertainty in hydrologic modelling. Yet, the scope of producing probabilistic
17 inflow forecasts in this study is limited to attaching a certain probability to the deterministic
18 forecasts so common in the Norwegian hydropower industry based on analysis of the statistical
19 properties of the error series from the conceptual model, and assessing its degree of reliability.
20 In the next section, the complementary model setup is formulated and the performance
21 evaluation criteria are provided. An example application is presented in the subsequent section.
22 This includes description of the study area and data used, findings from the evaluation of the
23 complimentary setup and its components during calibration and validation, and results of
24 forecasting skill assessment using deterministic and reliability metrics. Finally, concluding
25 remarks are provided.

26

27 **2 Methodology**

28 **2.1 The conceptual model setup**

29 The widely applied conceptual hydrologic model—HBV—(Bergström, 1995) is used in this
30 study. The version used allows dividing the study catchment up to 10 elevation zones. A
31 deterministic HBV model with already calibrated model parameter values was assumed to take

1 the role of the operational hydrologic models Norwegian hydropower companies commonly
 2 use for forecasting reservoir inflows. In the operational setup, the air temperature and
 3 precipitation input over the forecast lead-time are obtained from the Norwegian Meteorological
 4 Institute (www.met.no). As this study aims to improve hydrologic forecasts into the
 5 hydropower reservoirs by complementing the conceptual model by an error model, we assume
 6 that the predictions from the HBV model are made using as good quality input data as possible.
 7 Hence, the observed air temperature and precipitation data are used as input forecasts in
 8 hindcast.

9 **2.2 The complementary error model**

10 The error model aims at exploiting the bias, persistence and heteroscedasticity in the residuals
 11 and estimating the errors likely to occur in the forecast lead-time. Forecasting the error in the
 12 lead-time is regarded as a two-step process: off-line identification and estimation of the error
 13 model, and error predictions based on most recent information.

14 **2.2.1 Identification of the model structure**

15 An error model that captures the structures the processes model is missing should lead to a zero-
 16 mean-homoscedastic residual series from the modelling framework. In order to identify the
 17 right structure and establish a parsimonious model that adequately describes the data, we
 18 diagnose the residuals and address the bias, persistence and heteroscedasticity the series might
 19 exhibit as follows.

20 First and foremost, we transform the observed (Q) and the predicted (\hat{q} , from the conceptual
 21 model) inflows into z and \hat{z} , respectively. This way we deal with the heteroscedasticity seen
 22 in the residuals by making repeated use of Eq. 1 with the appropriate inflow term.

$$23 \quad \hat{z}_t = \begin{cases} \left((\hat{q}_t + \beta)^\lambda - \beta \right) \lambda^{-1} & \lambda > 0 \\ \log(\hat{q}_t + \beta) & \lambda = 0 \end{cases} \quad (1)$$

24 where β and λ are the transformation parameters.

25 The discrepancy (ε) between the observed and predicted inflow at time step (t) can be
 26 expressed as $\varepsilon_t = z_t - \hat{z}_t$. Analysis of whether the residuals are random or show some bias
 27 follows. Lest the mean of the residuals would be different from zero, the mean error (μ_e) is

1 subtracted from the error series (ε) to produce a zero-mean residual series ($e_t = \varepsilon_t - \mu_e$). This
 2 is followed by assessment of the auto correlation function (acf) and partial autocorrelation
 3 function (pacf), which are keys for identifying the order of Markovian dependence the residuals
 4 exhibit. We consider an autoregressive (AR) model structure (Eq. 2) to represent the persistence
 5 structure in the residual series. Comparative assessment of error models of different complexity
 6 would be an interesting work but is beyond the scope of this study. Xiong and O'Connor (2002)
 7 affirm that AR model's longstanding popularity is deservedly right and further emphasize
 8 effectiveness of a very parsimonious model such as AR model for error forecasting.

$$9 \quad \hat{e}_t = \sum_i^p a_i e_{t-i} \quad (2)$$

10 where p designates the length of the lag-time, and a_1, a_2, \dots, a_p are coefficients of the AR
 11 model.

12 In order to provide improved hourly reservoir inflow forecasts over a 24 hours lead-time, the
 13 error-forecasting model takes the form of Eq. (3). In order to overcome lack of observed
 14 residuals encountered for forecast lead-time (f) longer than one-step ahead, it is necessary to
 15 utilize estimated errors as inputs (see Eq. 3). The number of estimated errors values to be used
 16 as inputs depends on the identified order of the AR model and can vary across the forecast lead-
 17 times.

$$18 \quad \hat{e}_{t+f} = \begin{cases} \sum_{i=1}^p a_i e_{t+f-i} & \text{for } f = 1 \\ \sum_{i=1}^{f-1} a_i \hat{e}_{t+f-i} + \sum_{i=f}^p a_i e_{t+f-i} & \text{for } f \geq 2 \text{ and } p \geq f \\ \sum_{i=1}^p a_i \hat{e}_{t+f-i} & \text{for } f \geq 2 \text{ and } p < f \end{cases} \quad (3)$$

19 In its complete form, the error-corrected reservoir inflow forecast (z') from the complementary
 20 modelling framework can be given as

$$21 \quad z'_{t+f} = \hat{z}_{t+f} + (\mu_e + \hat{e}_{t+f}) \quad (4)$$

2.2.2 Parameter Estimation

Parameters of the AR model can be set to the corresponding Yule-Walker estimates of a_1, a_2, \dots, a_p given the autocorrelation function of the error series fulfils a form of linear difference equation. However, in practice, Eq. (2) can be treated as a linear regression and parameters can be estimated by Least Squares method as demonstrated by Xiong and O'Connor (2002). An iterative algorithm suggested in Beven et al. (2008) is adopted for estimating the model parameters while optimizing transformation of the inflow data. Adoption of a methodology that amalgamates parameter estimation and Box-Cox (Box and Cox, 1964) inspired transformation of inflow is useful for taking into account the heteroscedastic residuals and obtaining a normally distributed residual series from the error model. The parameter and inflow transformation steps with a little modification from Beven et al. (2008) over the calibration period $(1, \dots, T)$ are as follows:

1. Select values of $\beta, \lambda > 0$ and transform the reservoir inflows $(\hat{q}_{1:T}, Q_{1:T})$ to get $(\hat{z}_{1:T}, z_{1:T})$ using Eq. 1.
2. Calculate the residuals series from the transformed inflow data $(\varepsilon_{1:T} = z_{1:T} - \hat{z}_{1:T})$.
3. Perform an optimization for the error model parameters (a_1, a_2, \dots, a_p) to minimize $\sum (\varepsilon_{1:T} - \hat{\varepsilon}_{1:T})^2$, where $\hat{\varepsilon}$ represents the forecast from the error model which at a given observation time step (t) equals $(\mu_e + \hat{e}_t)$. Thus, the observed (ε) and forecasted $(\hat{\varepsilon})$ errors at a given observation time step (t) can be related as $\varepsilon_t = \hat{\varepsilon}_t + \eta_t$, where η_t is a random noise that describes the total uncertainty originating from various sources.
4. Adjust (β, λ) and repeat the optimization until the residuals of the error model appear homoscedastic. The η_t term (step 3) is assumed to be unimodal, symmetric and unbounded random variable with a zero expected-mean and second moment given as σ^2 .

2.3 Performance evaluation

In addition to visual evaluation of the hydrographs, performance of the present procedure is robustly analysed using deterministic and reliability metrics. The root mean square error

1 (*RMSE*), relative error (*RE*) and the Nash-Sutcliffe efficiency (*NSE*) (Nash and Sutcliffe, 1970)
 2 are employed to evaluate efficiency of the models during calibration and validation
 3 deterministically. Evaluations are made with respect to varying forecast lead-times and season
 4 wise as well. Among the three statistical performance criteria, the *RE* (Eq. 5) measures the
 5 relative error between the total observed and predicted inflow volume. For a good simulation the
 6 value of *RE* is expected to be close to zero. Quantifying the relative error (*RE*) of the
 7 simulations/forecasts is important because it indicates how the inaccuracies affect a hydropower
 8 company's ability to deliver the amount of energy it has pledged to provide to the energy
 9 market. Therefore, special attention is given to the less aggregate version of *RE*, which we
 10 hereon refer to as percentage volume error (*PVE*) and describe as follows.

$$11 \quad RE = \frac{\sum (z_t - \hat{z}_t)}{\sum z_t} \times 100\% \quad (5)$$

12 The *PVE* designates the relative error at each time step, which in reference to Eq. 5 can be
 13 obtained by omitting aggregation of the errors by summation. It indicates the magnitude of the
 14 errors as percentage of the observed inflows at each inflow time step. From hydropower systems
 15 operations point of view, the *PVE* enables evaluation of the forecast errors at each time step
 16 and assess implication on the power production capacity directly. The *PVE* analysis devised
 17 here divides the computed *PVEs* into six *PVE* classes (i.e. $\leq 10\%$, 10-20%, 20-30%, 30-40%,
 18 40-50% and $>50\%$), and treats overestimates and underestimates separately. The number of
 19 times each of the six absolute *PVE* classes appeared in the set or subset of interest (i.e.
 20 hydrologic year or seasons) is constructed by keeping score of the *PVE* class into which each
 21 and every residual fell in. Then the fraction of time each *PVE* class occurred is divided to the
 22 total number of points in the given set/subset and is reported as a percentage. This is designated
 23 as a “*PVE* count”. Model performance assessment using *PVE* (during simulation and
 24 forecasting) mainly focuses on assessing the change in number the number of incidences in
 25 each *PVE* set, which in other words means the change in *PVE* counts. The *PVE* count/change
 26 in *PVE* count, along with the above-mentioned deterministic statistical criteria, is used for
 27 evaluating simulation and forecasting skill of the complementarily setup system (conceptual
 28 model + error model). As a metric for measuring relative improvement in forecasting skills,
 29 high *PVE* counts for the low *PVE* classes (e.g. $\leq 10\%$) is considered desirable quality. The
 30 justification is that, the penalty a power producer incurs when failing to deliver the pledged

1 amount of power would be lesser if its forecasting system makes errors of lower PVE classes
2 more frequently.

3 Another useful metric used for assessing forecasting skill of the complementary setup is through
4 uncertainty analysis. An interval forecast (Chatfield, 2000) can be constructed by specifying an
5 upper and lower limit between which the future reservoir inflow is expected to lie with a certain
6 probability ($1-\alpha$). The prediction interval for the inflow forecast are estimated using the
7 Linear Regression Variance Estimator (LRVE) Shrestha and Solomatine (2006) describe.
8 Xiong et al. (2009) outline several indices that can serve for describing the properties of
9 prediction bounds of particular probability and for comparative study of prediction intervals
10 resulting from different uncertainty assessment schemes. The indices characterise the prediction
11 bound either by: the percentage of observations it contains, its band-width, or its symmetry
12 relative to the observation. According to Xiong et al. (2009), of all indices the containing ratio
13 (*CR*), which describes the percentage of observed inflows falling in the desired interval
14 percentage, is the widely used metrics for assessing reliability of probabilistic forecasts. We
15 adopt the *CR* metric for describing the reliability of the forecasts with the desired interval
16 percentage of 95% ($\alpha = 0.05$). Beside the *CR*, we verify the probabilistic forecasts graphically
17 using the less formal PIT uniform probability plot. The working procedure along detailed
18 application examples can be found in Laio and Tamea (2007) and Thyer et al. (2009). Among
19 others, Pokhrel et al. (2013) and Wang et al. (2009) demonstrate viability of the ‘PIT uniform
20 probability plot’ approach for checking uniformity (and investigating the causes, in cases of
21 deviations from uniformity) without binning the data subjectively.

22

23 **3 Example application**

24 **3.1 Study area and data**

25 The Krinsvatn catchment is located in Nord Trøndelag County in mid-north Norway. It
26 comprises an area of 207 km² and about 57% of the catchment is mountain area above
27 timberline. The elevation ranges from 87 to 628 m above mean sea level and is drained by the
28 Stjørna/Nord River. The dominant land use is forest covering 20.2% of the study site while
29 marsh, lakes and farmlands cover about 9%, 6.7% and 0.4% of the catchment area, respectively.
30 Figure 1 provides location and main characteristics of the study site, and the daily potential
31 evapotranspiration values used.

1 Observed hourly data of eleven water-years (2000/01 to 2010/11) was split into three sets used
2 for warming-up (2000/01), calibrating (2001/02-2005/06) and validating (2006/07-2010/11)
3 the conceptual and the error models alike. Observed precipitation and temperature data of two
4 meteorological stations (i.e. Svar-Sliper and Mørre-Breivoll) in neighbouring catchments are
5 used. Discharge data for the catchment is derived from water level records at the Krinsvatn
6 gauge station. Beven (2001) outlines the advantages to direct use of water level information in
7 hydrologic forecasting. Rating curve uncertainties and their influence on the accuracy of flood
8 predictions have been documented very well (e.g. Sikorska et al. 2013; Aronica et al., 2006;
9 Pappenberger et al. 2006; Petersen-Overleir et al. 2009). Krinsvatn is considered a stable
10 discharge measurement site with few external influences, and the rating curve was updated in
11 2004. This study, however, considers the uncertainty of the rating-curve to be one of the factors
12 contributing to the total error expressed in Eq. 2 and does not address it separately.

13 **3.2 HBV model for Krinsvatn catchment**

14 The catchment is divided into 10 elevation zones in the HBV model setup. Input data used are
15 hourly areal precipitation, air temperature, and potential evapotranspiration. The model is run
16 on an hourly time step for water years 2000/01 to 2005/06 with the last five water years being
17 used for model calibration. Calibration is carried out using the shuffled complex evolution
18 algorithm (Duan et al., 1993), with the *NSE* between the observed and predicted flows as an
19 objective function. Description of the model parameters along the corresponding optimized
20 values is provided in Table 1.

21 **3.2.1 Overview of the conceptual model's performance**

22 The simulation and observed reservoir inflow hydrographs shown in Fig. 2 indicate a certain
23 level of agreement for most of the calibration and validation periods, which the statistical
24 evaluations (Table 2) agree with. The overall hourly reservoir inflow predictions during
25 calibration and validation show efficiency of $NSE > 0.5$ and $RE < \pm 25\%$; even though
26 simulations match observations better during calibration than validation. High *NSE* values ($>$
27 0.8) during both calibration and validation reveal that the inflow simulations fit the observed
28 hydrographs best in the winter seasons. Nevertheless, it is evident that model predictions in the
29 validation period are prone to underestimation bias ($RE > 0$). Season wise assessment of the
30 validation period reveals the conceptual model's tendency to underestimate reservoir inflows

1 in spring and summer considerably. In light of what the *NSE* and *RE* metrics suggest, the lower
2 RMSE values (i.e. for instance summer season) do not reflect superior model performances.

3 PVE counts of the six PVE classes (i.e. $\leq 10\%$, 10-20%, 20-30%, 30-40%, 40-50% and $>50\%$)
4 are computed on the residuals between observed and simulated reservoir inflows. The stacked-
5 columns of Fig. 3a&b show how frequently each of the six absolute PVE classes occurred over
6 the calibration and validation period. The results reveal a large degree of discrepancy between
7 observations and predictions during calibration and validation. Simulated inflows deviated from
8 the corresponding observed values by a magnitude of more than $\pm 10\%$ in about 83.3%
9 (calibration) and 88.6% (validation) of the respective simulation time steps. Huge difference
10 between observations and simulations is noted in the summer season with absolute PVE of the
11 class $>50\%$ occurring in more than half of the simulation time steps throughout the calibration
12 and validation periods. Winter simulations listed the highest level of occurrence of PVE of the
13 class $\leq \pm 10\%$ during both calibration and validation. Comparable to the results in Table 2,
14 volume errors in winter simulations do not seem to be a serious problem, probably because the
15 season is predominantly a snow accumulation rather than runoff generation period. Errors of
16 the high absolute PVE classes scored high PVE counts in the spring and autumn seasons.

17 Details of the extent to which the reservoir inflows are under- and over-estimated can be seen
18 in Fig. 3c&d. The fraction of time the simulated inflows exhibited under- and over-estimation
19 during calibration is 51.9% and 46.8%, respectively. In the validation period, the reservoir
20 inflows are underestimated about 65.6% of the time compared to overestimation in 33.4% of
21 the times. This is also revealed in the findings from statistical metrics in Table 2, which disclose
22 the bias in the model. Yet, the results in Fig. 3 further reveal that the model predictions deviate
23 from the observations at high discharges. For example, during the validation period 59.2% of
24 the times observations exceeded the predictions by magnitudes more than 10%. Such
25 information is useful because direct evaluation of observed and predicted values explains the
26 implications of model performance on the planning and operation of a hydropower system
27 better than an aggregated variance based statistic. From an operational management point of
28 view, considerable underestimation of reservoir inflows can have both short- and long-term
29 effects on the operation of a hydropower system. In the short-term, the company could be forced
30 to release unvalued water especially when the reservoir water level is close to its maximum
31 capacity. Hence, the high percentage of underestimations that occur in the autumn and spring
32 seasons (during calibration and validation) should not be tolerated because the inflows in the

1 autumn and spring seasons are very important. On the one hand, substantial overestimation of
2 reservoir inflows can at least expose any Norwegian hydropower company to undesirable
3 expense due to obligations to match the power supply it has failed to deliver by dealing with
4 other producers in the intra-day physical market (Elbas). Although overestimation does not
5 seem to be a pertinent issue, Fig. 3d unmask that the inflows are overestimated by a magnitude
6 >50% at least 10% of the time in all seasons.

7 **3.2.2 Residual analysis**

8 Following the example of Xu (2001), a Kolmogorov-Smirnov test is applied to residuals of the
9 conceptual model. The test revealed that the residuals are not normally distributed. The
10 maximum deviation between the theoretical and the sample lines is 0.130, which is larger than
11 Kolmogorov-Smirnov test statistic of 0.008 at significance level $\alpha = 0.05$.

12 Presence of homoscedasticity in the residuals series is diagnosed visually by plotting the
13 residuals versus the predicted reservoir inflows (Fig. 4a). With respect to the horizontal axis,
14 the scattergram does not remain symmetric for the entire range of predicted inflows. The
15 residuals show high variability and possible systematic bias when inflows are less than 3.5mm
16 while the opposite is true when the inflows exceed 3.5mm. Inflows of magnitudes between 3.5
17 and 5.5mm seem to be underestimated while overestimation is visible when the inflow rates are
18 greater than 5.5mm. However, as can be seen from Fig. 2, inflows of magnitude up to 3mm
19 represent reservoir inflows during the rise of the hydrographs including all peak inflows for all
20 hydrologic years but 2005/2006 and 2010/2011. Hence, except for the possible systematic bias
21 during low flows, the inference from the scatterplot is inconclusive to support or dismiss the
22 issue of predominant underestimation revealed in the model performance evaluation. Moreover,
23 hourly inflows of magnitudes higher than 3mm are rare and occurred about 0.1% of the times
24 over the calibration and validation period.

25 Plots of autocorrelation and partial autocorrelation functions of the residual time series (Fig.
26 4b&c) indicate a strong time persistence structure in the error series. Rapid decaying of the
27 partial autocorrelation function confirms the dominance of an autoregressive process, which
28 the gradually decaying pattern of the autocorrelation function also suggests. Thus, in order to
29 obtain a Gaussian series it is important to address issues of heteroscedasticity and serial
30 correlation in the residual series. As the current study aims at utilising the persistent structure
31 in the residuals for supplementing the forecasting system, the corrective action to be taken only

1 aims at removing the heteroscedasticity. A successful way to do it is through transformation of
2 the flow data (e.g. Engeland et al., 2005). As outlined in the methodology section, the reservoir
3 inflows (both observed and predicted) are transformed while estimating parameters of the error
4 model.

5 **3.3 Structure and performance of the error model**

6 In accordance with the findings from the ACF and PACF plots discussed in section 3.3.2, AR
7 models of up to order $p = 3$ were investigated while estimating parameters of the error model.
8 As outlined in section 2.2.2, coefficient of the AR(p) model and the transformation parameters
9 were estimated by minimizing the sum of the squares of the offsets between the inflows
10 (observed and predicted) in the transformed space, and assessment of whether the subsequent
11 residuals from the complementary modelling framework appear homoscedastic and exhibited
12 correlation. The latter was assessed using the Kolmogorov-Smirnov (*KS*) statistic as a relative
13 quantitative measure followed by visual inspection of the residual plots, which led to the
14 selection of an AR(1) model with transformation parameters $\beta = 41.4$ and $\lambda = 0.9$, bias
15 correction $\mu_e = 0.021$ and coefficient $a_1 = 0.97$.

16 Calibration efficiencies calculated for the error model using the *RMSE*, *RE* and *NSE* metrics are
17 0.096, -100% and 0.517, respectively. Corresponding values for the validation period are
18 computed as 0.095, 20.3% and 0.630, respectively. *NSE* values for the calibration and validation
19 periods imply ability of the error model to capture at least half of the discrepancies observed
20 between observations and predictions from the conceptual model. All the three metrics reveal
21 a higher efficiency in the validation set than the calibration set. With reference to Table 2, this
22 suggests too much fitting of the HBV model to the data that led to extraction of more
23 information from the calibration set. Assessment of the residuals from the complementary
24 framework reveals that the transformation reduced the maximum deviation between the
25 theoretical and the sample lines slightly from 0.13 to 0.10; yet the residuals are not normally
26 distributed (i.e. Kolmogorov-Smirnov statistic of 0.008 at significance level of $\alpha = 0.05$). This
27 implies that the assumption the residuals from the complementary forecasting system would be
28 Gaussian is far from being true. As the aim of this study is to utilize the error and
29 complementary models additively, we discuss in the next section the extent to which the
30 complementary setup boosted prediction ability in the forecasting mode and come back to the

1 issue of violation of the Gaussian assumption in section 3.5, where we analyse the reliability of
2 the forecasts probabilistically.

3 **3.4 Forecasting skill of the complementary setup (deterministic assessment)**

4 Imitating operational application of forecasting models in the Norwegian hydropower system,
5 reservoir inflows for the day-ahead market (Elsport) are estimated using the presented
6 forecasting system. The system has to run once a day at an hourly time step, sometime before
7 12 pm after retrieving the latest observations, and the inflow forecasts are issued for the next
8 24 hourly time steps beginning from 12 o'clock noon. Overall performance of the
9 complementary model in forecasting the reservoir inflows during the calibration and validation
10 periods is first discussed and is followed by evaluation of its forecasting skill with respect to
11 forecast lead-times. Evaluation of the forecast skill presented in this paper is based on
12 assessment of forecasts made for the period between 2006/07 and 2010/11 as the datasets from
13 2000/01 to 2005/06 are used for calibrating the system.

14 **3.4.1 Overall performance**

15 Assessment of the overall forecasting skill of the complementary setup shows significant
16 improvement in forecast accuracy. The *RMSE* and *NSE* statistical criteria computed between
17 forecasted and observed inflows are 0.095 and 0.896, respectively. *RMSE* values for the
18 autumn, winter, spring and summer forecasts are 0.094, 0.090, 0.132 and 0.044, respectively,
19 and the corresponding *NSE* values are 0.904, 0.905, 0.859 and 0.873.

20 Proving capability of the complementary setup to reduce the bias revealed in the simulation
21 forecasts from the conceptual model, which was pointed out in the previous section, the 24
22 hours lead-time forecasts exhibited low-level underestimation bias with RE equal to 3.8%.
23 Degree of bias in the inflow forecasts differed seasonally. RE computed for each season in a
24 decreasing order is, summer (10.2%), spring (4.6%), autumn (2.9%) and winter (0.7%). The
25 relatively higher bias in the spring and autumn forecasts can be related to runoff generation in
26 the Krinsvatn catchment due to snow melting or occurrence of precipitation in the form of
27 rainfall, which can affect the persistence structure in the residual series obtained from the
28 conceptual model.

29 Stacked-column plots in Fig. 5 display the occurrence level of each of the six PVE classes in
30 the residual series between forecasts and observations. Visual comparison of stacked-column

1 plots of Fig. 5 and Fig. 3 shows reduction in PVE count of the high PVE classes and increase
2 in PVE counts of low PVE classes; e.g., PVE count for the PVE class $>\pm 50\%$ decreased by
3 about 15% while PVE count for the PVE class $\leq \pm 10\%$ grew by about 50%. In order to assess
4 this assertion, a further assessment is carried out by dividing the six PVE classes into two
5 groups: low PVE ($PVE \leq \pm 10\%$) and high PVE ($PVE > \pm 10\%$). Ratio between seasonal PVE
6 counts of the low and high PVE classes is taken and comparison is made on two sets of residual
7 series. These sets of residuals are, (1) residuals from the simulated forecasts (conceptual model),
8 and (2) residuals from forecasts of the complementary setup. Results are presented in Table 3.
9 Apart from confirming the success in reducing PVE counts of high PVE errors, the results
10 indicate that equal level of success is not achieved in all four seasons. In relative terms, high
11 PVE errors occur more often in the spring and summer forecasts. As pointed out earlier, this
12 can be associated to the snowmelt and, to a certain degree, to rainfall incidents occurring in
13 these seasons.

14 **3.4.2 Forecast skill with respect to forecast-lead times**

15 Relative reductions in *RMSE* between forecasts from the complementary setup and the
16 simulated forecasts from the conceptual model are computed. Detailed results for each season
17 of the hydrologic years between 2006/07 and 2010/11 are presented in Table 4. The results are
18 also summarized in terms of the minimum, mean and maximum relative *RMSE* reduction as
19 shown in Fig. 6. Excluding forecasts in autumn and winter seasons of 2006/07, relative *RMSE*
20 reductions are observed in forecasts of short and long lead-times. Of course, in all four seasons,
21 the achieved level of improvement in forecast accuracy is high for short lead-times and
22 diminishes gradually with increased lead-time. Results show that accuracy of the reservoir
23 inflows in the spring and summer seasons are improved over the entire range of the forecast
24 lead-time. Likewise, reduction in *RMSE* is observed for all autumn and winter inflow forecasts
25 except for years 2006/07 and 2007/08, respectively.

26 In order to get insight on the improvement level in a unit directly related to hydropower
27 production, the change in PVE count of each PVE class is calculated. Change in PVE count of
28 a given absolute PVE classes is the difference between the PVE counts for the complementary
29 setup and that for the conceptual model. The results are summarized as shown in Fig. 7. The
30 figure shows that the PVE count of high magnitude absolute PVE classes are reduced and the
31 opposite is true for that of the smaller absolute PVE classes. For instance, regardless of the type
32 of discrepancy (under- or over-estimation) noted, the change in PVE counts of the absolute *PVE*

1 of the class $>50\%$ is negative. The negative sign implies less errors falling in this PVE class in
2 the residual series from the complementary setup than those from the conceptual model.
3 Similarly, the changes in PVE counts of the 20-30%, 30-40% and 40-50% absolute PVE classes
4 indicate lowered fraction of occurrence of errors of these orders. In both cases of under- and
5 over-estimation, absolute *PVE* of the class $\leq 10\%$ occurred more frequently; for example, the
6 fraction of time reservoir inflow forecasts of 1 hour lead-time deviated from the observations
7 by a magnitude $\leq 10\%$ increased by about 52.7 and 27.7% during under- and over-estimations.
8 Overall, the plots show that the magnitude of discrepancy at each forecasting point is
9 significantly reduced. The improvement level at each forecast lead-time is proportional to the
10 vertical distance from the horizontal axis. It can be noted that, the vertical distance narrows
11 down with increasing lead-time suggesting a declining improvement level with increased lead-
12 time.

13 Calculation of the relative RMSE reduction and the change in PVE counts agree that the
14 forecast accuracy is improved through the complementary setup. The assessments further
15 revealed that the degree of improvement weakens with increased forecast lead-time. However,
16 the relative RMSE reduction computations indicate that in some occasions the simulated inflow
17 forecasts stand out to be better. The relative RMSE reduction values for lead-times longer than
18 20 hours (Table 4) show that complementing the conceptual model with an error model is
19 counterproductive in autumn and winter seasons of years 2007/08 and 2006/07, respectively.

20 **3.5 Reliability of the inflow forecast**

21 Computation of the containing ratio (*CR*) for the entire forecast reveals that 96% of the
22 observations are inside the 95% prediction interval. The inflow hydrographs (Fig. 8) confirm
23 that most of the observed inflows are contained in the specified uncertainty bounds.

24 The percentage of observation points falling within the 95% prediction interval varies from
25 season to season and across hydrologic years (see Fig. 9a). All observed winter and summer
26 inflows are bracketed in the 95% uncertainty bound at least 95% of the time. In general, the
27 winter season is more of a snow accumulation period and a closer observation of the
28 hydrographs (see Fig. 8) reveals that the summer hydrographs cover the recession and base flow
29 portions of the annual hydrographs. Thus, better persistence structure and predictable
30 discrepancies between simulated forecasts from the conceptual model and the observations. As

1 Goswami et al. (2005) argue, the persistence structure in residual series primarily arises from
2 the dynamic storage effects of a catchment system.

3 The desired percentage of autumn observations is contained in the 95% prediction interval in
4 the years 2006/07, 2008/09 and 2010/11. In the years 2007/08 and 2009/10, however, only 93
5 and 94% of the observed autumn inflows are bracketed in the estimated 95% prediction
6 intervals, respectively. Reliability score (*CR*) calculations for the spring season indicate that
7 percentage of observation points falling in the desired prediction interval percentage are below
8 95% except in the hydrologic years 2007/08 and 2008/09. Unlike winter and summer inflows,
9 autumn and spring flows mostly cover portions of the hydrograph corresponding to the rising
10 limb or high flow regime (see Fig. 8). While physical factors contributing to the increase in
11 quick flow into the reservoir are precipitation incidents (in the form of rainfall) and melting of
12 snow in the headwaters, comprehension of this concept and its encapsulation into the HBV
13 model leaves control of the catchment response to two threshold values (TX and TS, see Table
14 1 for description). Employing such simple threshold values to govern initiation of the runoff
15 generation process based on air temperature measurement at a given time-step obviously
16 involves more sources of uncertainty (i.e. measurement, model structure and model
17 parameters). For instance, we assume the input air temperature at a given time step is
18 erroneously recorded to be higher than TX and/or TS due to measurement error. Subsequently,
19 the model will partition the precipitation as rainfall and initiate melting of snow, which the
20 observation does not reveal. This kind of misclassification of precipitation and/or
21 misrepresentation of snow accumulation and melting processes can simply occur due to the
22 error in the input temperature record. Because of this, the persistence in the errors between
23 simulated forecasts from the conceptual model and the observations can get weaker. According
24 to Goswami et al. (2005), some degree of persistence in the model input (i.e. rainfall) is another
25 primary source of the persistence characteristic of observed flow series. Even though the least
26 *CR* calculated for the autumn and spring seasons are by no means too bad (i.e. 93% and 90%,
27 respectively), the requirement for reliability is for the uncertainty bound to contain as much
28 fraction of observations as desired percentage of prediction interval; hence, the complementary
29 setup presented seems to have struggled with it.

30 The fraction of observed inflows bounded within the estimated prediction interval decreases
31 with increased lead-time (Fig. 9b). Reliability score for lead-times up to 17 hours fulfil the

1 requirement of containing 95% of the observations. For lead-times beyond 17 hours, the
2 reliability declines and reaches 92% at forecasts lead-time of 24 hours.

3 Findings from evaluation of the forecast skill of the complementary setup using deterministic
4 and probabilistic metrics support each other. The present procedure is able to improve accuracy
5 of reservoir inflow forecasts and the level of improvement decreases as the forecast lead-time
6 increases. Deterministic evaluation of performance of the forecast system indicates that the
7 concept of complementing the conceptual model with a simple error is not always effective. As
8 discussed earlier, in some occasions the present method can get counterproductive in
9 forecasting inflows when the forecast lead-time is beyond 20 hours. Similarly, detailed
10 assessment of the reliability (Table 5) shows that the *CR* of the forecasting system can get below
11 95% at forecast lead-times less than 17 hours; e.g. at forecast lead-time of 9 hours only 89% of
12 the observed spring inflows of year 2006/07 are bracketed in the 95% prediction interval. It can
13 also be noted that for shorter forecast lead-times, the percentage of observations contained in
14 the prediction bounds exceed 95%. Although a greater proportion of observations falling in the
15 prediction bound is desirable, a high *CR* at short forecast lead-times might indicate a too wide
16 band-width. This along a *CR* that declines with increased lead-time might suggest invalidity of
17 the assumptions behind computation of the bounds (e.g. Smith et al., 2012). The two issues at
18 stake here are the Gaussian assumption on the basis of which the prediction bounds were
19 constructed, and the model identification and parameter estimation approach implemented.
20 ~~However, the results from the PIT uniformity probability test (Fig. 9c-f) confirm that the~~
21 ~~distribution of the forecasts from the complementary framework are consistent with the~~
22 ~~observed inflow. The PIT plots of the observed inflows almost plot along the diagonal bisector~~
23 ~~and remain within the Kolmogorov 5% significance in cases of slightly deviations.~~In order to
24 assess the former, we conducted the PIT uniformity probability test. From operational
25 hydrology point of view, we concur with the opinion of Thyer et al. (2009) that the toughest
26 goodness-of-fit test the complementary framework has to pass is whether the predictive
27 distribution is consistent with the observed inflow, which the PIT uniform probability plots
28 evaluate directly. ~~With regard to the model assumptions, we recall~~At each time step we derived
29 p-value of the observation from the corresponding predictive distribution and constructed
30 empirical cdf of the p-values (i.e. different sets based on season, lead-time, etc.). Comparison
31 of these empirical cdf of the p-values with that of a uniform distribution (Fig. 9c-f) reveal that
32 the uncertainty attached to the deterministic forecasts is imperfect. Overall, PIT uniformity
33 probability test confirms that the uncertainty is overestimated significantly irrespective of

1 season and lead-time. In relative terms, significance of the overestimation reduces with
2 increased lead-time. PIT plots of the spring season show a relatively lower uncertainty
3 overestimation, even though they neither plot along the diagonal bisector nor remain within the
4 Kolmogorov 5%. This might explain that the cause of the uncertainty overestimation could be
5 use of a high standard deviation relative to the inflow magnitude occurring throughout the year.
6 However, this finding of “uncertainty overestimation” clearly contradicts the lower than
7 expected percentage of coverage the CR metrics revealed. This along with evidences of the
8 need to truncate the lower tails of the prediction bound, and recalling from the Kolmogorov-
9 Smirnov test (section 3.3) that the residuals from the error forecasting model did not honour the
10 homoscedasticity assumption even after transformation, ~~which~~ might suggest invalidity of the
11 model assumption. According to Schoups and Vrugt (2010), in hydrologic applications residual
12 series are often assumed to be independent and identically distributed but these assumptions are
13 usually violated. In the next section, we briefly assess reliability of the model identification and
14 parameter estimation approach implemented in this study.

15 **3.6 On the implemented parameter estimation technique**

16 The parameter (AR model coefficient(s) and transformation parameters) estimation technique
17 we employed (section 2.2.2) follows a pseudo multi-objective optimization approach, which
18 includes minimizing the sum of squares of the residuals and making sure a homoscedastic
19 residual series. We first employed the Least Square (LS) method to estimate the parameters
20 associated to several AR models (of orders 1 to 3). Since the unit of the inflows (the errors as
21 well) in the transformed space depended on the transformation parameters, and the inclusion of
22 the transformation parameters into the calibration problem posed a challenge to identify the
23 optimal among the candidate AR models, we resorted to the dimensionless Kolmogorov-
24 Smirnov (KS) statistic. The KS metric served as a relative quantitative measure to discriminate
25 between candidate models by measuring how close-to-constant the residual variances' are. As
26 a result, the selected AR model is suboptimal in terms of yielding the least discordance between
27 predictions and observations. Putting aside the issue of (in)validity of the Gaussian assumption,
28 we demonstrate that shortcomings of the present LS and KS (LS-KS) model the probabilistic
29 metrics revealed are not unique to the implemented parameter estimation approach. In order to
30 verify this, we setup an AR model estimated the coefficients and transformation parameters by
31 maximizing the Gaussian maximum likelihood (GML).

1 An AR(2) model was identified with coefficients and transformation parameters: $\beta = 1.08$,
2 $\lambda = 0.01$, $a_1 = 1.82$ and $a_2 = -0.82$. All the deterministic metrics used in this study confirm
3 performance improvement of a slight degree by the GML based model during calibration and
4 validation. This does not come as a surprise because parameters of the LS-LK based model
5 were suboptimal. On the other hand, the KS test revealed that the maximum distance between
6 the sample line and the theoretical line increased to 0.290, which is higher than the statistic the
7 error transformation using parameterization of the LS-KS model (0.10) yielded. To be fair,
8 comparison of the KS statistics associated to the GML and LS-LK transformation parameters
9 might not be appropriate because the LS-KS based AR model was selected for its low KS
10 statistic. Nevertheless, the KS statistic corresponding to the GML based transformation shows
11 a heteroscedasticity of degree higher than the untransformed residuals (0.13). The PIT uniform
12 probability plots ~~assured~~revealed that both approaches significantly overestimated the
13 ~~distribution of the predictions matches the observation very well~~uncertainty in a similar pattern.
14 Comparison of the *CR* of the GML and LS-LK based models showed a similar proportion of
15 observations contained in the prediction interval. The *CR* again reveals the same characteristics
16 of high values at short lead-times and the fraction of observations contained in the prediction
17 bound declines at longer lead-times. This affirms that validity of the Gaussian assumptions
18 stand out as the main issue requiring further investigation in relation to probabilistic assessment.

19

20 **4 Concluding remarks**

21 In the present study, the forecasting system comprising additively setup conceptual and simple
22 error model is presented. Parameters of the conceptual model were left unaltered, as are in most
23 operational setups, and the data-driven model was arranged to forecast the corrective measures
24 to be made to outputs of the conceptual models to provide more accurate inflow forecasts into
25 hydropower reservoirs several hours ahead.

26 Application to the Krinsvatn catchment revealed that the present procedure could effectively
27 improve forecast accuracy over a 24 hours lead-time. This proves that the efficiency of a flow
28 forecasting system can be enhanced by setting up a data-driven model to complement a
29 conceptual model operating in the simulation mode. Furthermore, the current study reveals that
30 analysing characteristics of the residuals from the conceptual model is important and
31 heteroscedastic behaviour should be addressed before identifying and estimating parameters of

1 the error model. Compared to past studies that applied data-driven and conceptual models in a
2 complementary way, the present procedure is successful in providing acceptably accurate
3 forecast for extended lead-times. It also outlines procedure for extracting useful information
4 from the bias, the persistence and the heteroscedasticity the residual series from the conceptual
5 model exhibited, although the assumption that the residuals from the modelling framework to
6 be random failed to hold.

7 Results also indicate that probabilistic forecasts can be obtained from deterministic models by
8 constructing uncertainty of the complementary setup based on predictive uncertainty of the
9 simple error model. The uncertainty bound seems to satisfy the reliability requirement when
10 evaluated over the entire forecasting period. Its reliability with respect to forecast lead-time also
11 appears satisfactory for lead-times up to 17 hours. Nevertheless, the season wise assessment
12 revealed that the degree of reliability of the forecasts vary from season to season. Given that
13 the error model essentially makes use of the persistence structure in the residuals from the
14 conceptual model, the present procedure seems to be unable to capture transitions in the
15 hydrograph errors from over- to under-estimation (and vice versa). On the one hand, it was
16 unveiled that the degree of reliability of the forecasts decline with longer lead-times and the
17 deterministic metrics (*RMSE* and *PVE*) confirmed the same.

18 In order to address these challenges, a future development can be to explore methodologies for
19 taking care of seasonal variability in the structure of the residual series. Updating the error
20 models periodically can be one solution but care must be taken if the selected updating method
21 makes a Gaussian assumption. Another alternative would be to explore more complex
22 stochastic models for the residuals, that use exogenous predictor variables either observed
23 directly (much like the seasonal reservoir inflow forecasting models described in Sharma et al,
24 2000), or using state variables simulated from the conceptual model (like the Hierarchical
25 Mixtures of Experts framework in Marshall et al, 2006 and Jeremiah et al, 2013). Formulation
26 of these models will also offer better insight into the deficiencies that exist within the HBV
27 conceptual model, thereby allowing further improvement to reduce the structural errors present.

28 A subsequent work (Gagne et al., 2015) attempts to address some of these issues using a filter
29 updating procedure, which assimilates inflow measurements periodically to the error-
30 forecasting model, and explores the potential of a data assimilation technique for improving
31 model forecast accuracy and constraining forecast uncertainty without significant
32 computational costs.

1 Another interesting topic of future investigation is the intercomparison of the probabilistic
2 forecasts presented in the current paper with the same from popular methods such as Bayesian
3 forecasting system (BFS), the generalized likelihood uncertainty estimation (GLUE) and the
4 Bayesian recursive estimation (BaRE). We believe this would enable identification of the most
5 effective and reliable probabilistic forecasting method that can also be implemented in an
6 operational setup.

7

8 **Acknowledgements**

9 This work was supported by the Norwegian Research Council through the project Updating
10 Methodology in Operational Runoff Models (192958/S60) and the consortium of Norwegian
11 hydropower companies led by Statkraft. The hydrological data used in the project were
12 retrieved from database of the Norwegian Water Resources and Energy Directorate (NVE). The
13 meteorological data were obtained from Trønderenergi AS and we thank Elena Akhtari for
14 making them available to us. We would like to acknowledge the assistance of Professor Keith
15 Beven in the preparation of this manuscript.

16

1 **References**

- 2 Abebe, A. J. and Price, R. K.: Managing uncertainty in hydrological models using
3 complementary models, *Hydrolog. Sci. J.*, 48(5), 679-692, 2003.
- 4 Aronica, G. T., Candela, A., Viola, F., and Cannarozz, M.: Influence of rating curve uncertainty
5 on daily rainfall - runoff model predictions, *Predictions in Ungauged Basins: Promise and*
6 *Progress*, 303, 116-124, 2006.
- 7 Bergström, S.: The HBV model, in: *Computer Models of Watershed Hydrology*, edited by:
8 Singh, V.P., Water Resources Publications, Highlands Ranch, CO., 443-476, 1995.
- 9 Beven, K.: *Environmental Modelling: An Uncertain Future?*, Taylor and Francis Group,
10 London and New York, 2009.
- 11 Beven, K.: *Rainfall-runoff modelling: The primer*, 2nd ed., Wiley-Blackwell, Chichester, 2012.
- 12 Beven, K. J., Smith, P.J., and Freer, J.: So just why would a modeller choose to be incoherent?,
13 *J. Hydrol.*, 354, 15-32, 2008.
- 14 Box, G.E.P. and Cox, D.R.: An analysis of transformations. *J. Roy. Stat. Soc. B Met.*, 211-252,
15 1964.
- 16 Chatfield, C.: *Time-series forecasting*, CRC Press, 2000.
- 17 Engeland, K., Xu, C.-Y., and Gottschalk, L.: Assessing uncertainties in a conceptual water
18 balance model using Bayesian methodology, *Hydrolog. Sci. J.*, 50(1), 45-63, 2005.
- 19 Goswami, M., O'Connor, K. M., Bhattarai, K. P., and Shamseldin, A. Y.: Assessing the
20 performance of eight real-time updating models and procedures for the Brosna River, *Hydrol.*
21 *Earth Syst. Sc.*, 9(4), 394-411, 2005.
- 22 [Gragne, A.S., Alfredsen, K., Sharma, A., Mehrotra, R.: Recursively updating the error-](#)
23 [forecasting scheme of a complementary modelling framework for enhancing accuracy of](#)
24 [reservoir inflow forecasts, *J. Hydrol.*, 527, 967-977, 2015.](#)
- 25 Jeremiah, E., Marshall, L., Sisson, S. A., and Sharma, A.: Specifying a hierarchical mixture of
26 experts for hydrologic modeling: Gating function variable selection, *Water Resour. Res.*, 49(5),
27 2926-2939, 2013.
- 28 Kachroo, R. K.: River flow forecasting: Part 1 - A discussion of the principles, *J. Hydrol.*, Vol.
29 133, 1-15, 1992.

- 1 Krzysztofowicz, R.: Bayesian theory of probabilistic forecasting via deterministic hydrologic
2 model, *Water Resour. Res.*, 35(9), 2739-2750, 1999.
- 3 Krzysztofowicz, R.: The case for probabilistic forecasting in hydrology, *J. Hydrol.*, 249(1-4),
4 2-9, 2001.
- 5 Li, L., Xu, C. Y., and Engeland, K.: Development and comparison in uncertainty assessment
6 based Bayesian modularization method in hydrological modeling. *J. Hydrol.*, 486, 384-394,
7 2013.
- 8 Laio, F., and Tamea, S.: Verification tools for probabilistic forecasts of continuous hydrological
9 variables, *Hydrol. Earth Syst. Sci.*, 11(4), 1267 – 1277, 2007.
- 10 Liu, Y., Weerts, A. H., Clark, M., Hendricks Franssen, H.-J., Kumar, S., Moradkhani, H., Seo,
11 D.-J., Schwanenberg, D., Smith, P., van Dijk, A. I. J. M., van Velzen, N., He, M., Lee, H., Noh,
12 S. J., Rakovec, O., and Restrepo, P.: Advancing data assimilation in operational hydrologic
13 forecasting: progresses, challenges, and emerging opportunities, *Hydrol. Earth Syst. Sci.*, 16,
14 3863–3887, doi:10.5194/hess-16-3863-2012, 2012.
- 15 Madsen, H. and Skotner, C.: Adaptive state updating in real-time flow forecasting—a combined
16 filtering and error forecasting procedure, *J. Hydrol.*, 308, 302-312, 2005.
- 17 Marshall, L., Sharma, A., and Nott, D. J.: Modelling the Catchment via Mixtures: Issues of
18 Model Specification and Validation, *Water Resour. Res.*, 42, W11409,
19 doi:10.1029/2005WR004613, 2006.
- 20 Moll, J. R.: Real time flood forecasting on the River Rhine, in: *Proceedings of the Hamburg*
21 *Symposium on Scientific Procedures Applied to the Planning, Design and Management of*
22 *Water Resources Systems*, IAHS Publ. no. 147, 265-272, 1983.
- 23 Montanari, A. and Brath, A.: A stochastic approach for assessing the uncertainty of rainfall-
24 runoff simulations. *Water Resour. Res.*, 42, 40(1), W01106, 2004.
- 25 Nash, J. and Sutcliffe, J.: River flow forecasting through conceptual models part I — A
26 discussion of principles, *J. Hydrol.* 10(3), 282-290, 1970.
- 27 Pappenberger, F., Matgen, P., Beven, K. J., Henry, J. B., Pfister, L., and De Fraipont, P.:
28 Influence of uncertain boundary conditions and model structure on flood inundation
29 predictions, *Adv. Water Resour.*, 29, 1430–1449, 2006.

1 Petersen-Overleir, A., Soot, A., and Reitan, T.: Bayesian Rating Curve Inference as a
2 Streamflow Data Quality Assessment Tool, *Water Resour. Manage.*, 23(9), 1835-1842, 2009.

3 Pokhrel, P., Robertson, D.E. and Wang, Q.J.: A Bayesian joint probability post-processor for
4 reducing errors and quantifying uncertainty in monthly streamflow predictions. *Hydrol. Earth
5 Syst. Sci. Discuss.* 9(10), 11199-11225, 2012.

6 Renard, B., Kavetski, D., Kuczera, G., Thyer, M., and Franks, S. W.: Understanding predictive
7 uncertainty in hydrologic modeling: The challenge of identifying input and structural errors,
8 *Water Resour. Res.*, 46, W05521, doi:10.1029/2009WR008328, 2010.

9 Roald, L. A., Skaugen, T. E., Beldring, S., Væringstad, Th., Engeset, R., and Fjørland, E. J.:
10 Scenarios of annual and seasonal runoff for Norway based on climate scenarios for 2030-49,
11 met.no Report 19/02 KLIMA, 2002.

12 Schoups, G. and Vrugt, J.A.: A formal likelihood function for parameter and predictive
13 inference of hydrologic models with correlated, heteroscedastic, and non-Gaussian errors.
14 *Water Resources Research* 46(10), 2010.

15 Serban, P. and Askew A.J.: Hydrological forecasting and updating procedures, *Hydrology for
16 the Water Management of Large River Basins*, IAHS Publ. n. 201, 357- 369, 1991.

17 Shamseldin, A.Y. and O'Connor, K.M.: A non-linear neural network technique for updating of
18 river flow forecasts, *Hydrol. Earth Syst. Sc.*, 5(4), 577-597, 2001.

19 Sharma, A., Luk, K. C., Cordery, I., and Lall, U.: Seasonal to interannual rainfall probabilistic
20 forecasts for improved water supply management: Part 2 - Predictor identification of quarterly
21 rainfall using ocean-atmosphere information, *J. Hydrol.*, 239(1-4), 240-248, 2000.

22 Shrestha, D.L. and Solomatine, D.P.: Machine learning approaches for estimation of prediction
23 interval for the model output. *Neural Networks*, 19(2), 225-235, 2006.

24 Sikorska, A. E., Scheidegger, A., Banasik, K., and Rieckermann, J.: Considering rating curve
25 uncertainty in water level predictions, *Hydrol. Earth Syst. Sci.*, 17, 4415–4427, 2013.

26 Smith, P. J., Beven, K. J., Weerts, A. H., and Leeda, D.: Adaptive correction of deterministic
27 models to produce probabilistic forecasts, *Hydrol. Earth Syst. Sci.*, 16, 2783–2799, 2012.

28 Solomatine D. P. and Shrestha D. L.: A novel method to estimate model uncertainty using
29 machine Learning techniques. *Water Resour. Res.*, 45, W00B11, 2009.

1 Thyer, M., Renard, B., Kavetski, D., Kuczera, G., Franks, S. W., and Srikanthan, S.: Critical
2 evaluation of parameter consistency and predictive uncertainty in hydrological modeling: a case
3 study using Bayesian total error analysis, *Water Resour. Res.*, 45, W00B14,
4 doi:10.1029/2008WR006825, 2009.

5 Todini, E.: Hydrological catchment modelling: past, present and future, *Hydrol. Earth Syst. Sc.*,
6 11(1), 468-482, 2007.

7 Toth, E., Brath, A., and Montanari A.: Real-time flood forecasting via combined use of
8 conceptual and stochastic models, *Physics and Chemistry of the Earth, B*, 24(7), 793-798, 1999.

9 Wang, Q. J., Robertson, D. E., and Chiew, F. H. S.: A Bayesian joint probability modeling
10 approach for seasonal forecasting of streamflows at multiple sites, *Water Resour. Res.*, 45,
11 W05407, doi:10.1029/2008WR007355, 2009.

12 World Meteorological Organization: Simulated real-time intercomparison of hydrological
13 models, WMO Pub., 241 pp, 1992.

14 Xiong, L. and O'Connor, K. M.: Comparison of four updating models for real-time river flow
15 forecasting, *Hydrolog. Sci. J.*, 47(4), 621-639, 2002.

16 Xiong, L. H., Wan, M., Wei, X. J., and O'Connor, K. M.: Indices for assessing the prediction
17 bounds of hydrological models and application by generalised likelihood uncertainty
18 estimation. *Hydrolog. Sci. J.*, 54(5), 852-871, 2009.

19 Xu, C-Y.: Statistical analysis of parameters and residuals of a conceptual water balance
20 model—methodology and case study. *Water Resour. Manage.*, 15, 75–92, 2001.

21

1 Table 1 Model parameters and corresponding optimized values.

Parameter	Description	Unit	Optimized value
Snow routine			
TX	Threshold temperature for rain/snow	[°C]	2.23
CX	Degree-day factor for snow melt (forest free part)	[mm/d°C]	9.95
CXF	Degree-day factor for snow melt (forested part)	[mm/d°C]	5.21
TS	Threshold for snow melt/freeze (forest free part)	[°C]	0.73
TSF	Threshold for snow melt/freeze (forested part)	[°C]	-1.80
CFR	Refreeze coefficient	[mm/d°C]	0.04
LW	Max relative portion liquid water in snow	[-]	0.085
Soil and evaporation routine			
FC	Field capacity	[mm]	306.87
FCDEL	Minimum soil moisture filling for POE	[-]	0.31
BETA	Non-linearity in soil water retention	[-]	3.84
INFMAX	Infiltration capacity	[mm/h]	30.22
Groundwater and response routine			
KUZ2	Outlet coefficient for quickest surface runoff	[1/day]	1.65
KUZ1	Outlet coefficient for quick surface runoff	[1/day]	0.99
KUZ	Outlet coefficient for slow surface runoff	[1/day]	0.42
KLZ	Outlet coefficient for groundwater runoff	[1/day]	0.09
PERC	Constant percolation rate to groundwater storage	[mm/day]	1.60
UZ2	Threshold between quickest and quick surface runoff	[mm]	122.34
UZ1	Threshold between quick and slow surface runoff	[mm]	49.97

2

1 Table 2 Summary of overall and seasonal performance of the conceptual model during the
 2 calibration (2001/02 to 2005/06) and validation (2006/07 to 2010/11) periods.

Seasons	Calibration period			Validation period		
	RMSE [mm]	RE [%]	NSE [-]	RMSE [mm]	RE [%]	NSE [-]
Overall	0.139	1	0.842	0.162	18.8	0.700
Autumn	0.147	1.8	0.724	0.147	11.3	0.769
Winter	0.182	-3.7	0.894	0.126	9.7	0.812
Spring	0.131	-2.7	0.709	0.246	24.6	0.509
Summer	0.073	28.2	0.641	0.079	38.2	0.592

3

1 Table 3 Ratio between occurrence frequency of low PVE ($\leq 10\%$) and high PVE ($> 10\%$) errors
 2 for the hydrologic years 2006/07-2010/11.

Data set	Overestimation				Underestimation			
	Aut.	Win.	Spr.	Sum.	Aut.	Win.	Spr.	Sum.
Simulated forecast (HBV model)	4.4	5.1	7.6	4.5	6.2	5.2	12.8	25.4
Forecast (complementary setup)	1.1	1.2	1.5	2.0	0.9	0.5	1.1	1.3

3

1 Table 4 Relative RMSE reductions (%) in reservoir inflows forecast as a function of forecast lead-time (* designates relative RMSE reduction
 2 of <0)

Season	Lead Time [hour]																								
	/year	1	2	3	4	5	6	7	8	9	10	11	12	13	14	15	16	17	18	19	20	21	22	23	24
Autumn	06/07	89.3	79.3	70.1	62.7	56.7	52.3	48.5	45	41.7	38.4	35	31.6	28.2	25.6	23.7	21.7	19.1	16.6	15.3	14.3	13.8	13	11.5	10.0
	07/08	91.6	84.4	78.6	73.5	67.6	62.2	58.0	53.8	50.7	48.0	44.8	41.4	38.8	36.3	33.8	30.7	26.3	19.5	10.9	3.3	*	*	*	*
	08/09	93.9	87.9	81.7	76.7	71.0	65.9	62.1	58.5	54.1	49.2	44	39.4	35.7	32.3	28.8	25.7	23.2	70	18.4	16.7	15.3	14.1	12.7	11.5
	09/10	90.9	83.2	76.9	70.9	64.7	59.1	54.9	51.0	47.2	44.2	41.1	38.1	35.1	30.0	29.5	27.1	25.1	23.3	21.9	70.0	70.0	10.0	19.1	18.4
	10/11	92.1	84.9	78.7	67.7	62.4	57	53.9	51.2	47.5	44.8	42.4	40.3	38	35.8	33.9	30.0	29.4	26.2	23.1	30.0	17.2	14.7	12.7	10.9
Winter	06/07	94.2	87.9	82.2	75.6	60.5	49.3	42.8	36.3	31.3	26.3	21.4	17.5	12.9	9.0	6.7	4.6	2.5	1.3	1.0	0.0	*	*	*	*
	07/08	91	81.9	73.3	66.2	59.9	54.1	49.2	44.8	40	36.1	33.3	30.8	28.1	25.4	23.2	90	19.5	17.5	15.6	15.5	16.5	17.5	18.1	18.4
	08/09	91.7	83.9	77.0	74.0	72.2	68.4	62.2	55.1	49.5	44.4	39.8	36	28.9	22.2	18.2	15.6	13.9	12.8	11.9	11.1	9.9	8.6	7.3	5.8
	09/10	94.9	91.4	87.3	83.5	80.3	78.8	76.7	72.7	65.9	58.1	51.8	46.9	43.4	40.2	37.7	35.5	33.7	32.2	30.9	29.4	27.8	26	24.1	22.2
	10/11	93.9	88.7	83.1	75.9	68.1	64.9	61.4	57.1	52.3	47	41.8	36.9	32.2	28.4	26	24.2	22.6	90	19.4	17.7	16	14.6	13	11.1
Spring	06/07	94.2	88.2	82.4	77	71.7	66.3	61.1	56.4	52.3	48.9	45.8	43.1	40.6	38.3	36	33.9	31.8	30	28.5	27.2	26.2	25.2	24.1	23.2
	07/08	96.6	93.3	89.8	86.2	82.6	79.0	75.6	72.8	70.4	68.4	66.6	64.9	63.1	61.3	59.4	57.6	55.8	54	52.5	51.1	49.7	48.4	47.1	46.0

	08/09	95	90.4	85.8	81.6	77.7	73.7	70.6	67.9	65.7	63.5	61.1	58.7	56.3	54	51.7	49.4	47	44.7	42.4	40.1	37.7	35.3	33.2	31.6
	09/10	93.9	87.7	81.7	76.0	70.6	64.9	59.3	54.4	50.6	47.4	44.8	42.5	40.4	38.5	36.8	35.2	33.9	32.8	30.0	31.3	30.5	29.7	29.0	28.3
	10/11	94.6	88.6	82.2	75.7	69.4	63.4	57.7	52.5	48.7	46.8	44.5	41.7	39.0	36.7	34.6	32.7	31.1	29.8	28.7	27.8	26.8	25.8	24.6	23.7
	06/07	94.8	90	85.7	82.8	80.1	76.3	72.6	69.7	67.4	66.0	65.1	63.7	60.1	58.2	56.3	54.2	51.6	49.6	47.6	44.9	42.2	39.5	36.8	34.4
	07/08	90.7	81.4	73.3	66.3	60.3	55.6	51.4	48.0	45.4	42.6	39.9	39.4	39.1	37.1	34.6	32.8	31.0	29.3	28.4	27.4	26.9	26.2	24.8	23.2
Summer	08/09	97.2	94.4	91.6	89	85.1	78.2	69.2	60.3	52.9	47.1	41.6	36.7	32.5	28.8	25.4	22.7	50.0	18.6	17.1	15.9	14.6	13.3	12.4	11.9
	09/10	92.4	84.8	79.1	76.2	74.2	71.5	68.4	65.2	61.0	57.1	54.3	51.9	50.0	47.7	45.1	43.0	41.1	39.3	37.0	35.8	35.0	34.1	33.2	30.0
	10/11	94.2	88.7	82.9	76.4	69.7	64.4	59.3	54.3	49.8	45.8	42.5	39.8	37.2	35.1	33.1	31.5	30.0	28.6	27.5	27.0	26.5	25.9	25.5	25.0

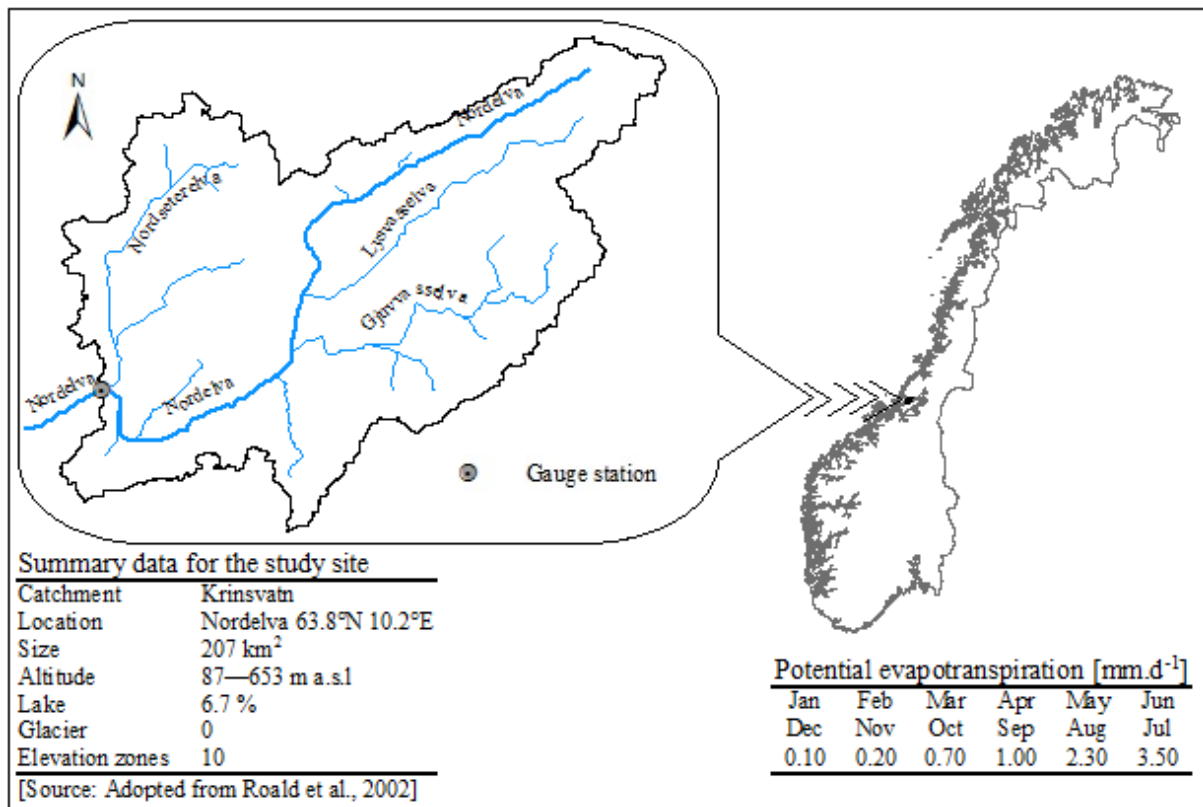
1

2

1 Table 5 Summary of seasonal containing ratio (95% prediction interval) during reservoir inflow forecasting (2006/07 to 2010/11)

Season	Lead Time [hour]																								
	/year	1	2	3	4	5	6	7	8	9	10	11	12	13	14	15	16	17	18	19	20	21	22	23	24
Autumn	06/07	99.9	99.9	97.8	97.8	97.8	97.8	97.8	97.8	97.8	97.8	96.7	94.5	94.5	93.4	93.4	93.4	93.4	90.1	90.1	91.2	90.1	90.1	89.0	89.0
	07/08	99.9	99.9	98.9	98.9	97.8	97.8	97.8	97.8	97.8	97.8	96.7	94.5	91.2	90.1	90.1	89	87.9	87.9	86.8	85.7	85.7	84.6	83.5	83.5
	08/09	99.9	99.9	99.9	99.9	99.9	98.9	98.9	95.6	95.6	95.6	95.6	95.6	95.6	95.6	95.6	95.6	94.5	93.4	93.4	93.4	92.3	92.3	91.2	90.1
	09/10	99.9	99.9	98.9	97.8	97.8	96.7	96.7	95.6	94.5	93.4	93.4	91.2	92.3	92.3	92.3	92.3	93.4	93.4	92.3	92.3	92.3	91.2	90.1	90.1
	10/11	99.9	99.9	99.9	98.9	98.9	97.8	98.9	98.9	97.8	96.7	95.6	95.6	95.6	95.6	95.6	95.6	95.6	94.5	93.4	93.4	93.4	92.3	92.3	91.2
Winter	06/07	99.9	99.9	99.9	99.9	97.8	96.7	96.7	95.6	95.6	95.6	95.6	95.6	94.4	94.4	93.3	93.3	92.2	92.2	92.2	92.2	91.1	91.1	91.1	90.0
	07/08	99.9	99.9	98.9	97.8	97.8	97.8	97.8	97.8	96.7	96.7	94.5	93.4	93.4	92.3	94.5	94.5	94.5	95.6	96.7	95.6	95.6	95.6	94.5	94.5
	08/09	99.9	99.9	99.9	99.9	98.9	98.9	98.9	97.8	97.8	97.8	97.8	97.8	97.8	95.6	95.6	95.6	95.6	94.4	94.4	94.4	94.4	94.4	95.6	95.6
	09/10	99.9	99.9	99.9	99.9	99.9	99.9	99.9	99.9	99.9	99.9	98.9	98.9	98.9	98.9	98.9	98.9	98.9	98.9	98.9	98.9	97.8	97.8	97.8	97.8
	10/11	99.9	99.9	99.9	99.9	98.9	96.7	96.7	96.7	96.7	96.7	96.7	96.7	96.7	95.6	95.6	96.7	95.6	95.6	95.6	95.6	94.4	94.4	94.4	94.4
Spring	06/07	99.9	99.9	98.9	98.9	97.8	95.7	94.6	93.5	89.1	89.1	89.1	89.1	90.2	88.0	88.0	88.0	88.0	88.0	87.0	85.9	84.8	84.8	84.8	83.7
	07/08	99.9	99.9	99.9	99.9	99.9	99.9	99.9	98.9	98.9	98.9	98.9	98.9	97.8	97.8	97.8	96.7	95.7	94.6	94.6	94.6	94.6	94.6	94.6	94.6
	08/09	99.9	99.9	98.9	98.9	98.9	98.9	97.8	97.8	97.8	96.7	96.7	96.7	96.7	96.7	96.7	96.7	95.7	95.7	95.7	93.5	93.5	93.5	93.5	92.4
	09/10	99.9	99.9	98.9	97.8	97.8	97.8	96.7	96.7	94.6	94.6	94.6	93.5	93.5	93.5	91.3	91.3	91.3	91.3	90.2	90.2	91.3	89.1	89.1	90.2

	10/11	99.9	98.9	98.9	96.7	96.7	95.7	94.6	93.5	92.4	92.4	90.2	90.2	89.1	88	89.1	87	85.9	85.9	84.8	83.7	83.7	83.7	82.6	82.6	
	06/07	99.9	99.9	99.9	99.9	99.9	99.9	99.9	99.9	99.9	99.9	99.9	99.9	99.9	99.9	98.9	98.9	98.9	98.9	98.9	98.9	97.8	97.8	97.8	97.8	97.8
Summer	07/08	99.9	99.9	99.9	99.9	98.9	98.9	98.9	98.9	98.9	98.9	98.9	98.9	98.9	98.9	98.9	98.9	98.9	98.9	98.9	98.9	98.9	98.9	98.9	98.9	98.9
	08/09	99.9	99.9	99.9	99.9	99.9	99.9	99.9	98.9	98.9	98.9	98.9	98.9	98.9	98.9	98.9	98.9	98.9	98.9	98.9	98.9	98.9	98.9	98.9	98.9	98.9
	09/10	99.9	99.9	99.9	99.9	99.9	99.9	99.9	99.9	99.9	99.9	99.9	99.9	99.9	99.9	99.9	99.9	99.9	99.9	99.9	99.9	98.9	98.9	98.9	98.9	98.9
	10/11	99.9	99.9	99.9	99.9	98.9	98.9	98.9	98.9	98.9	97.8	96.7	96.7	96.7	96.7	96.7	96.7	96.7	96.7	96.7	96.7	95.7	95.7	95.7	95.7	95.7

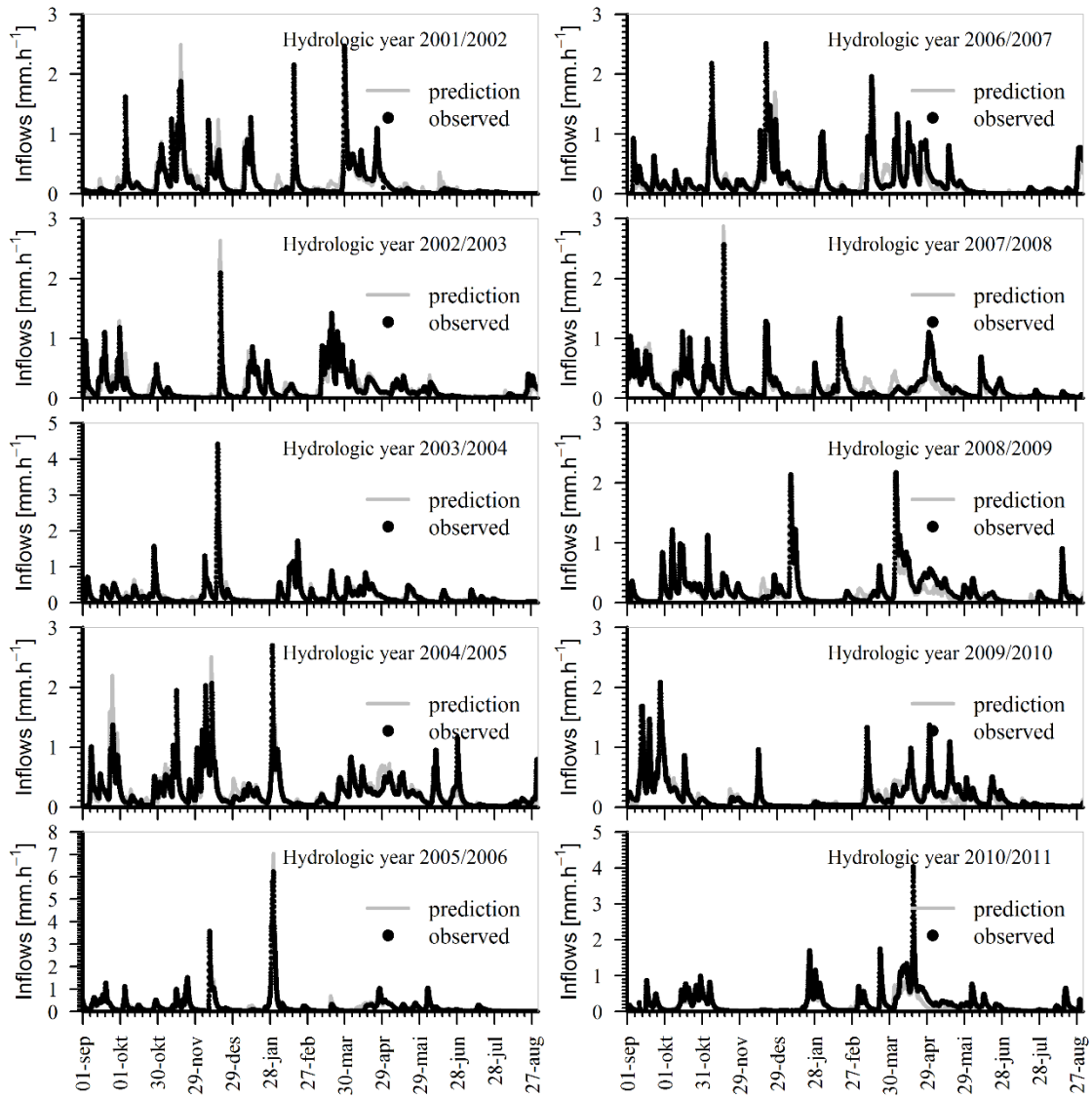


1

2

3 Figure -1. Location, characteristics and potential evapotranspiration estimates of the study

4 catchment.

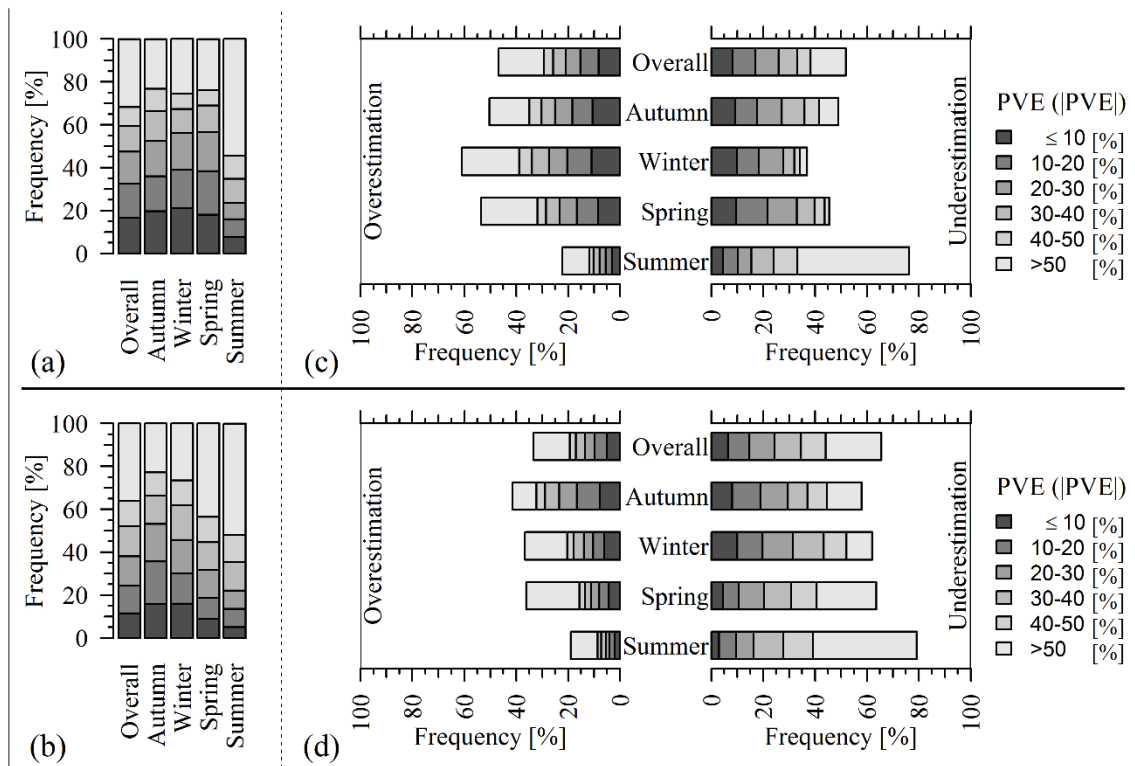


1

2

3 Figure 2. Observed and predicted reservoir inflow hydrographs during calibration (left column)

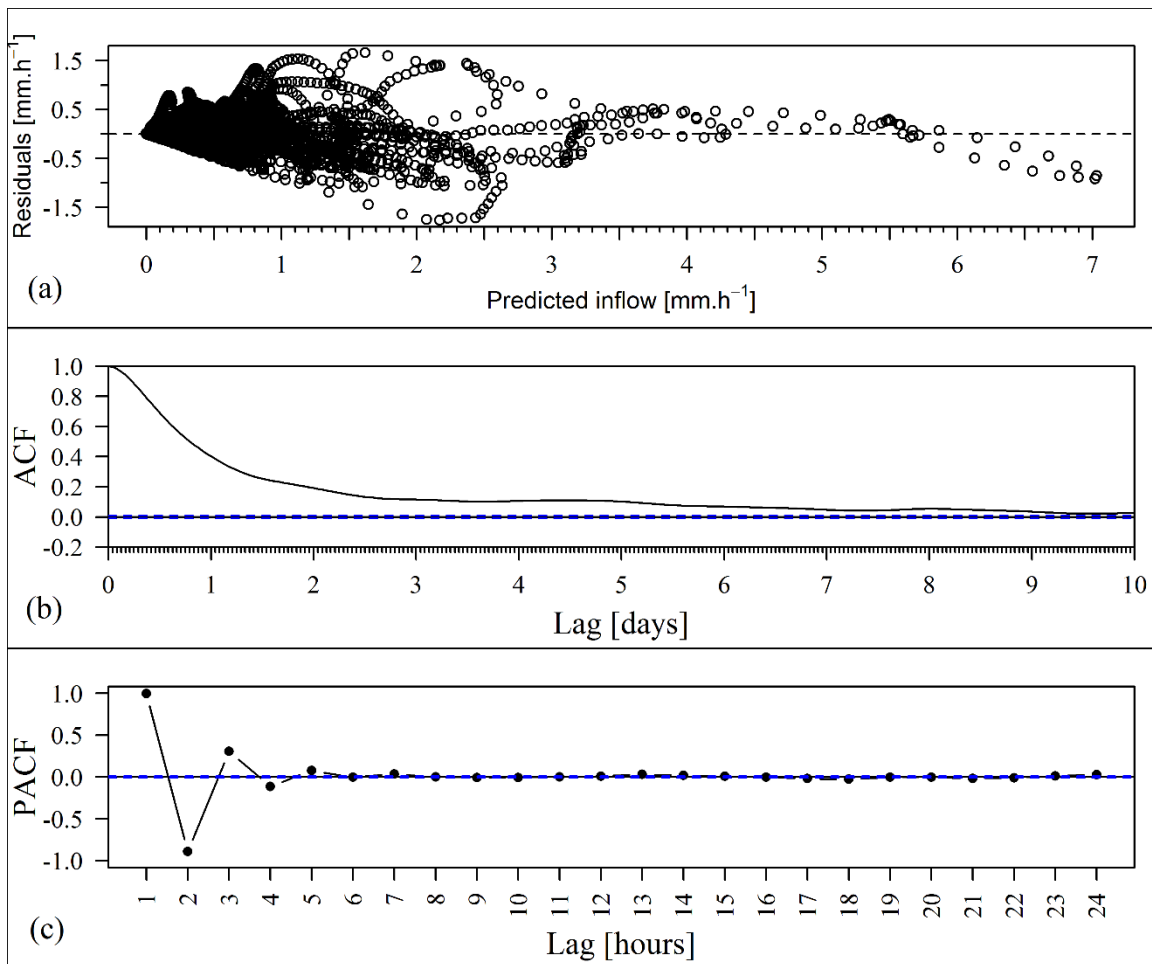
4 and validation (right column) of the conceptual model.



1

2

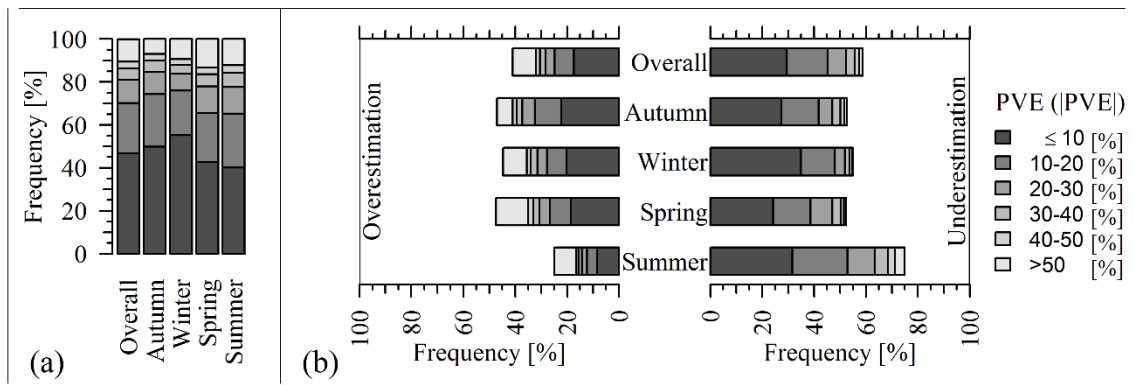
3 Figure 3. Stacked-column plots of: (1) PVE counts of the six absolute PVE classes ($\leq 10\%$, 10-
 4 20%, 20-30%, 30-40%, 40-50% and $>50\%$) during calibration (a) and validation (b); and (2)
 5 the fraction of times under- and over-estimation incidents corresponding to the six PVE classes
 6 occurred during calibration (c) and validation (d).



1

2

3 Figure 4. Plots of (a) residuals from the conceptual model as a function of predicted inflow
 4 during the calibration period, (b) autocorrelation function of the residuals, and (c) partial
 5 autocorrelation functions of the residuals.



1

2

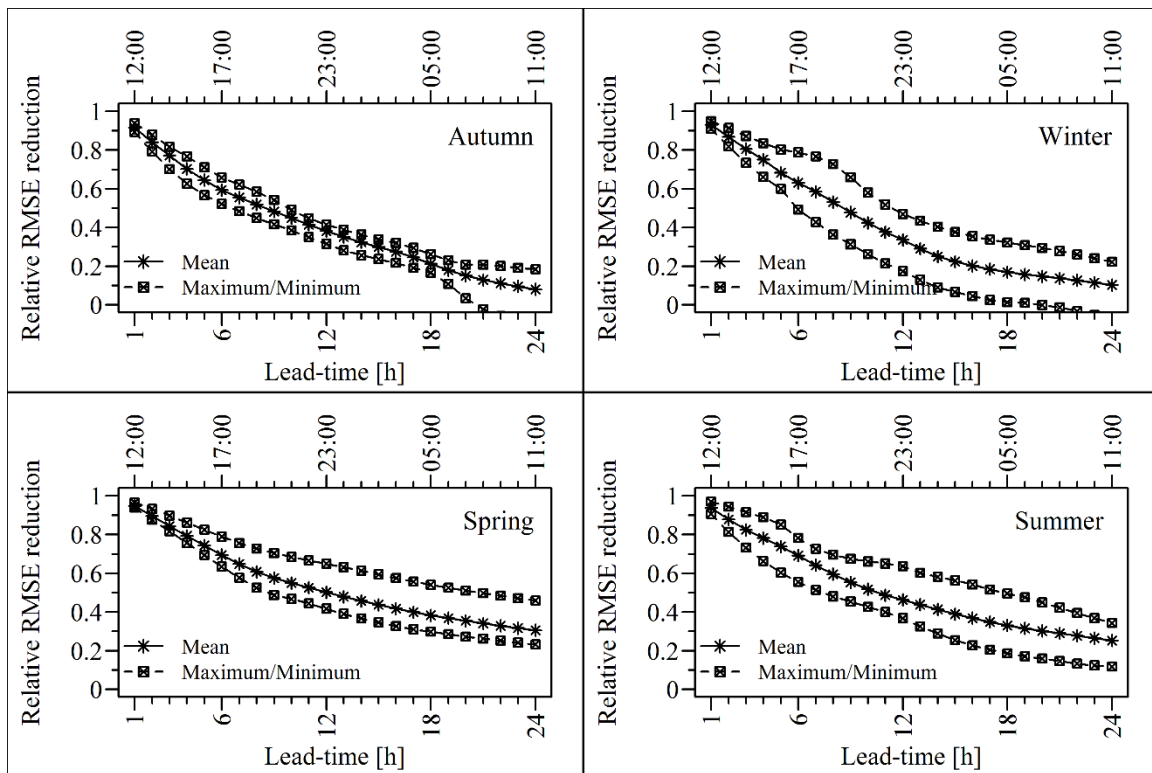
3

4

5

6

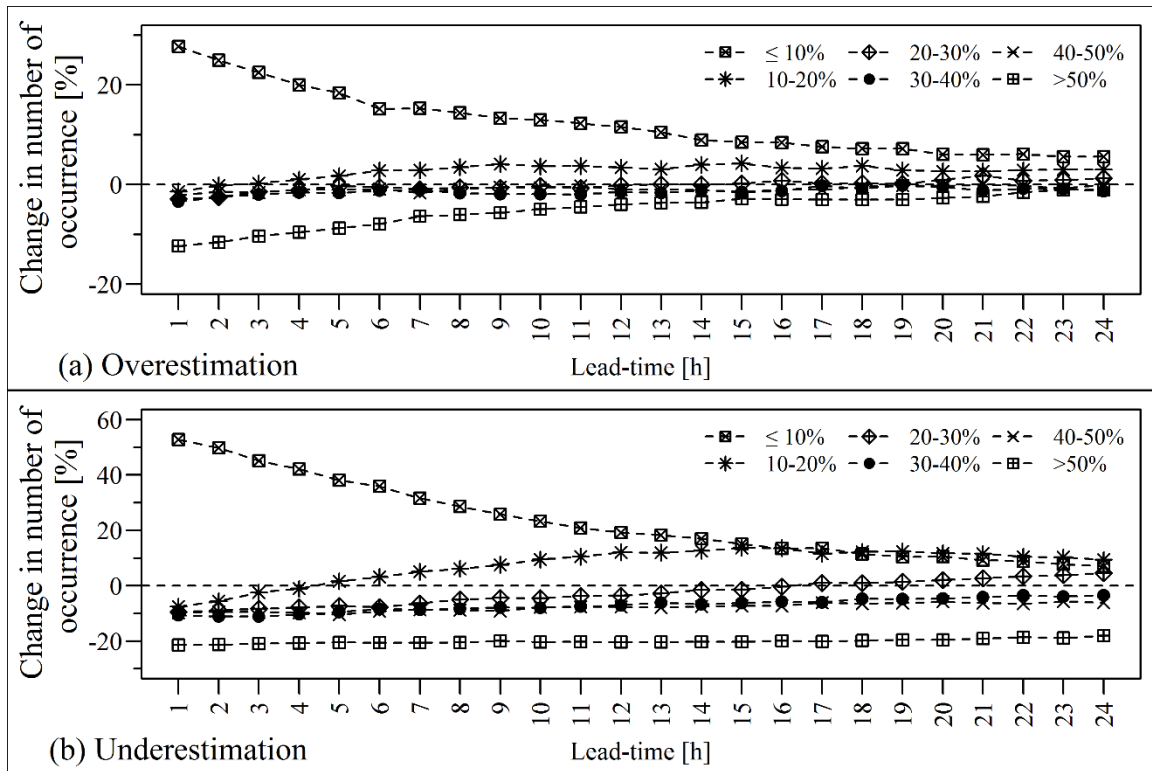
Figure 5. Stacked-column plots of: (a) PVE counts of the six absolute PVE classes ($\leq 10\%$, 10-20%, 20-30%, 30-40%, 40-50% and $>50\%$) observed in reservoir inflow forecasts from the complementary setup; and (b) the corresponding fraction of times under- and over-estimation incidents corresponding to the six PVE classes occurred. Hydrologic years 2006/07-2010/11.



1

2

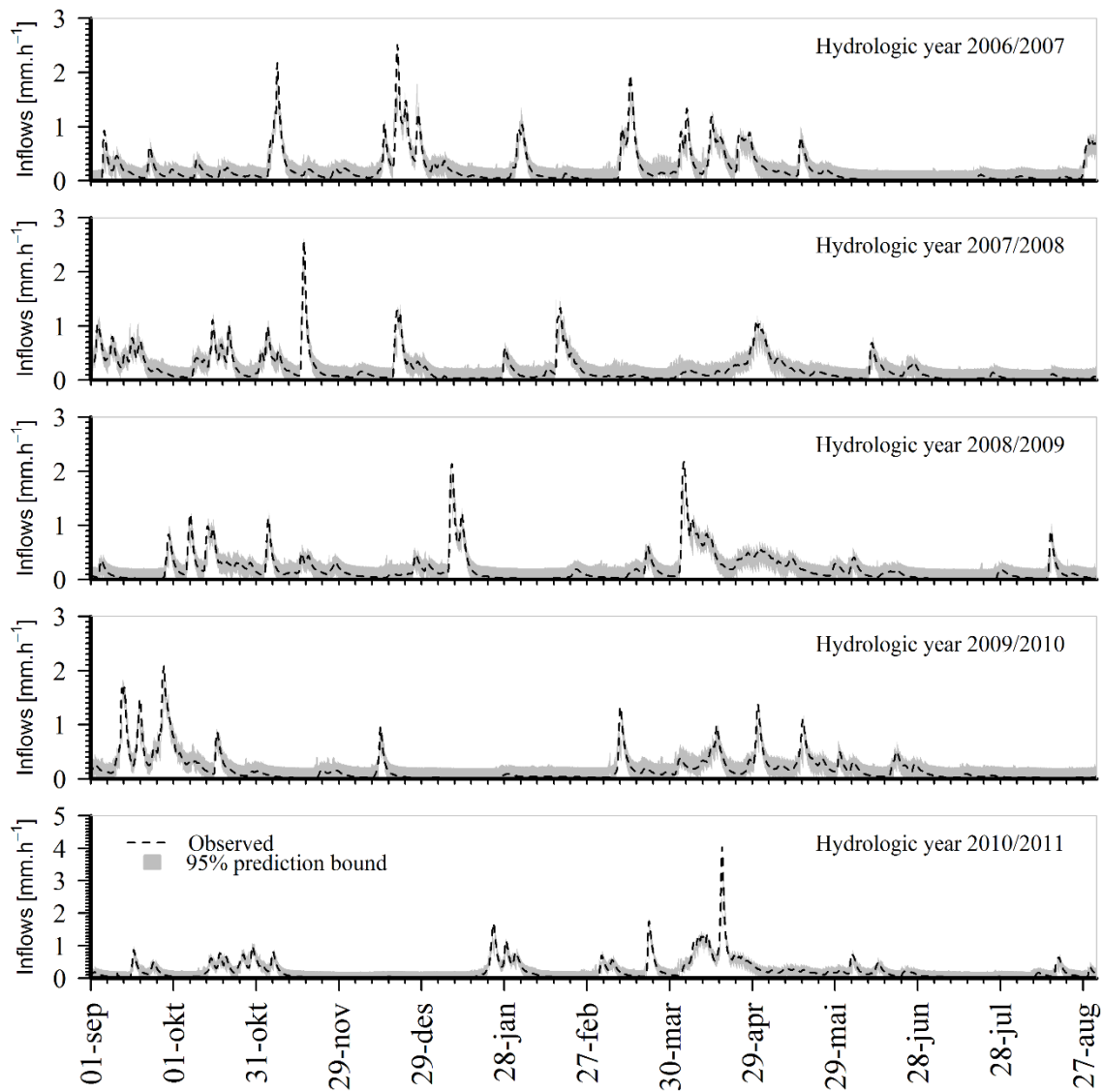
3 Figure -6. Summary of relative seasonal RMSE reductions as a function of forecast lead-time
 4 (minimum, mean and maximum values computed from corresponding computations for
 5 hydrologic years 2006/07 - 2010/11).



1

2

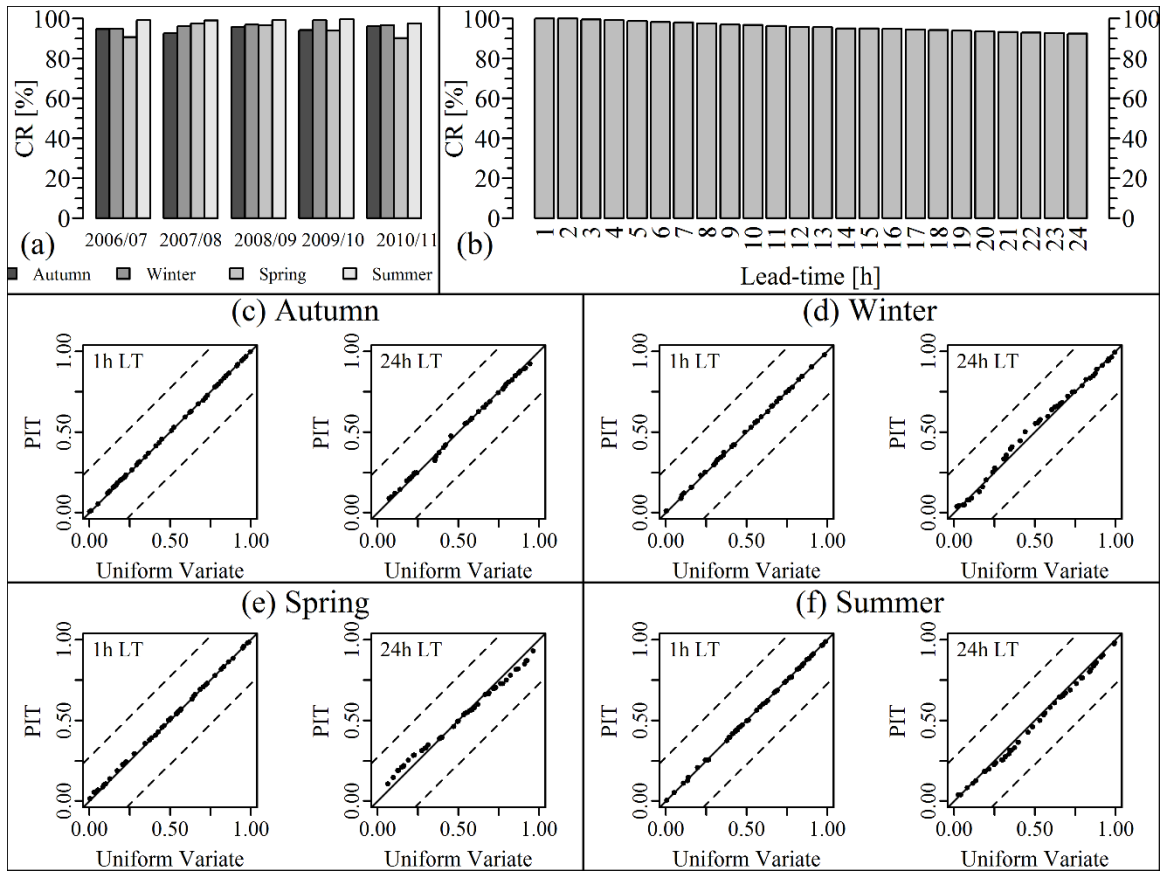
3 Figure 7. Change in number of occurrence of the six absolute PVE classes ($\leq 10\%$, 10-20%,
 4 20-30%, 30-40%, 40-50% and $>50\%$) as a function of forecast lead-time: (a) overestimation
 5 and (b) underestimation.



1

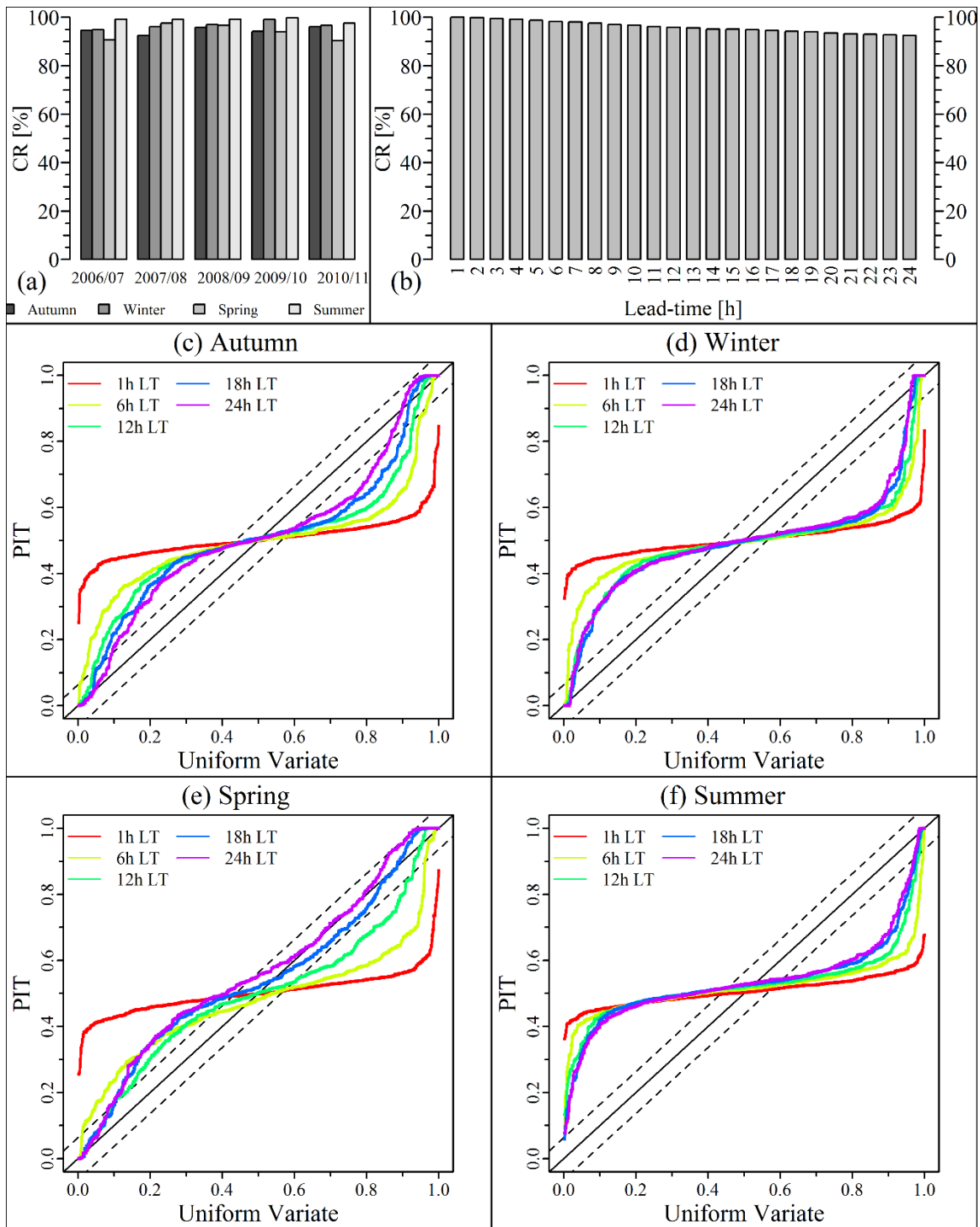
2

3 Figure 8. Observed hydrograph (broken lines) and the 95% prediction bound



1

2



1

2

3 Figure 9. Reliability score (containing ratio- CR) for 95% prediction interval for: (a) each
 4 season of every hydrologic year; and (b) different forecast lead-times based on entire series.
 5 Panels (c)-(f): sample PIT uniform probability plots for each of the four seasons at 1-hour, 6,
 6 12, 18 and 24 hour forecast lead-times. Solid line designates the theoretical uniform
 7 distribution, broken lines represent the Kolmogorov significance band, and the dots denote
 8 PIT value of the observed inflow-values.